Hydrology and Earth System Sciences, 3(2), *151–175* (1999) © EGS

Hydrology & Earth System Sciences

The pulsed migration of hydrocarbons across inactive faults

S.D. Harris,[1,2] L. Elliott[1] and R.J. Knipe[2]

[1] Department of Applied Mathematics, University of Leeds, Leeds, LS2 9JT, UK.
[2] Rock Deformation Research, School of Earth Sciences, University of Leeds, Leeds, LS2 9JT, UK.

Abstract

Geological fault zones are usually assumed to influence hydrocarbon migration either as high permeability zones which allow enhanced along- or across-fault flow or as barriers to the flow. An additional important migration process inducing along- or across-fault migration can be associated with dynamic pressure gradients. Such pressure gradients can be created by earthquake activity and are suggested here to allow migration along or across inactive faults which 'feel' the quake-related pressure changes; i.e. the migration barriers can be removed on inactive faults when activity takes place on an adjacent fault. In other words, a seal is viewed as a temporary retardation barrier which leaks when a fault related fluid pressure event enhances the buoyancy force and allows the entry pressure to be exceeded. This is in contrast to the usual model where a seal leaks because an increase in hydrocarbon column height raises the buoyancy force above the entry pressure of the fault rock. Under the new model hydrocarbons may migrate across the inactive fault zone for some time period during the earthquake cycle. Numerical models of this process are presented to demonstrate the impact of this mechanism and its role in filling traps bounded by sealed faults.

Introduction

The published literature on secondary migration of hydrocarbons considers that faults act in two primary ways to influence migration. Either they are assumed to be open pathways of high permeability or they are considered as barriers to the flow. An additional and important possibility, modelled here, is that hydrocarbons can migrate across or along inactive faults when quakes on an adjacent fault induce a pressure pulse that can promote migration of hydrocarbons across the inactive fault. In other words, the seal is viewed as a temporary barrier, or retardation feature, which leaks when a quake-related fluid pressure event allows the entry pressure of the fault rock material to be exceeded. This is in contrast to the normal model where a seal leaks because of an increase in hydrocarbon column, i.e. the buoyancy force exceeds the entry pressure of the fault rock. Under the new model, hydrocarbons may migrate across the inactive fault zone for the time period that the fluid pressure difference $(p_h - p_w)$ is above the critical entry pressure p_c, see Fig. 3.

Figures 1 and 2 provide a description of this system and show the basis for the numerical calculation of the amount of hydrocarbon that can be moved across a fault in this manner. This new model is based on the known importance of fluid pressure variations during faulting events. Pressure variations have been the foundation of many models which relate fluid flow to faulting processes. For example, when the fluid pressure exceeds the least principal stress by an amount equal to the strength of the rock, a hydrofracture can be generated or reactivated. This basis has been used to model fault pumping and valving (Sibson, 1981, 1992, 1996), earthquake propagation (Lockner and Byerlee, 1995) and top seal leaking (Holm, 1996; Larson *et al.*, 1992). The new model for migration proposed here differs in that it does not rely on fracturing or dilation to activate flow, but proposes that when the effect of buoyancy and fluid pressure pulses combine to exceed the entry pressure of seals then flow of hydrocarbon across/along the barrier is possible. In addition, many seals in hydrocarbon provinces are dynamic systems which are in equilibrium, or in a delicate balance of a leaking rate and a hydrocarbon influx rate controlling the accumulation columns. Such dynamic systems will be very sensitive to pulses which are above the background (or long term) fluid pressure levels, but are below the pressure levels needed to dilate and fracture flow barriers. Therefore, the role of pulses in fluid pressure gradients is critical. The cause of fluid pressure variations usually considered in migration studies is compaction driven or transformation controlled processes (Ge and Garven, 1994). It is proposed here that fault related pressure induced gradients also need evaluation and inclusion in models of hydrocarbon migration pathways. The dynamic model suggests that the migration

behaviour patterns in areas where fault systems are active depends fundamentally on the pressure level pulses and properties of the seals. Three levels of behaviour can be identified:

Level 1. Buoyancy control. $(p_h - p_w) \leq p_c$
Seal leaks in this case are primarily controlled by the buoyancy force at the top of the column alone. The buoyancy pressure needs to build up, by addition of hydrocarbon to a column, to the entry threshold pressure level before leakage occurs.

Level 2. Fault related pulsed flow.
$p_c < (p_h - p_w) < p_{frac}$
This is the condition for seal leakage associated with dynamic pressure changes without breaching by fracturing and is the basis of the model introduced here. The amount of leakage will be controlled by the time period when $(p_h - p_w) > p_c$.

Level 3. Open fracture/fault controlled flow.
$(p_h - p_w) \approx p_{frac}$
Here the seal fails by breaching because the mechanical strength of the seal is exceeded. Note that the failure mechanism may be either dilation of existing structures or generation of new structures (fracture and fault arrays).

The following points are important aspects of the pulsed flow across non-active faults during near-by fault activity:

(1) There is no need to wait ≈100,000 years for compaction related pressure cycles to allow cross seal leakage.

(2) Large numbers of pressure pulses are known to occur during fault activity. For example note the 500 quakes per day felt during the Matsushiro swarm (Sibson, 1996). Each of these will create a fluid pressure transient.

(3) This mechanism of leaking can operate away from active faults but within a volume affected by pressure pulses on an active fault. This creates a vision of fault-related fluid pressure transients propagating through a volume affected by a faulting event. The propagation of these pressure waves will be complex because the dampening and re-enforcement of the pressure wave will depend upon the three-dimensional permeability and porosity structure. Both sedimentological features (e.g. sand and shale body architecture and connectivity) and structural features (e.g. the size, shape and distribution of fault juxtaposition windows with different transmissivities) will contribute to the three-dimensional pattern of pressure histories within the volume. It is, therefore, likely that the shapes of the volumes which experience similar pressure levels, or rates of change of pressure, during a single event will be complex.

(4) The proposed pulsing mechanism may explain entry into hydrocarbon accumulations which are apparently bounded by sealed faults with no migration route into the reservoir.

(5) The timing of migration is often linked to faulting events but the subtle role of pressure cycling and flow across seals has not been considered before.

(6) The database collected by Rock Deformation Research during the last five years on the petrophysical properties on seals provides the platform for quantifying the impact of this pulsed leakage process.

(7) The proposed mechanism is not included in models of secondary migration. It should be. In addition, this mechanism should be added as a possible contribution to the fracture-leak models used to assess flow through top seals.

Controls and model basis

The important components of the proposed model of flow across inactive fault seals are listed below:

- The entry pressure characteristics of the fault.
- The magnitude and duration of each pressure event.
- The statistical distribution of population of pulse sizes over an extended time period.

Each of these aspects is discussed separately below.

THE ENTRY PRESSURE CHARACTERISTICS OF THE FAULT

Quantification of entry pressure data for fault rocks is vital to the modelling of flow across fault zones. During the last five years Rock Deformation Research has built its own computer controlled accurate permeameter (able to measure to $< 1\mu D$) and combined permeability data with mercury injection data on different fault rocks. This unique dataset now contains information on more than 400 fault rocks and has allowed determination of the relationship between entry pressures and permeability for fault rocks. A simplification of this relationship is used to evaluate pulsed flow across faults.

THE MAGNITUDE AND DURATION OF EACH PRESSURE EVENT

Schowalter (1979) reviewed the impact of hydrodynamic flow on seal behaviour and recognised how down dip flow increases the sealing capacity of a flow barrier and that up dip flow will reduce the sealing capacity. The critical factor is the alteration of the fluid pressure gradient with depth. The mechanism investigated here is where the depth/pressure gradient can be considered to be modified during a distant faulting event. The result is to induce a change in the buoyancy force which alters the sealing capacity of the inactive fault zone.

Accurate calculations for the pulse model requires information on the range of pressure changes which may be associated with faulting events and the time period over which these pulses operate. Data on the character of the pressure pulses comes from a number sources. For example, Parry and Bruhn (1990) report a fluid inclusion study from fault zones which indicate that fluid pressure transients of 5 MPa to 120 MPa occur on faults at a depth of

3–5 km. Information in Bruhn *et al.* (1990), Schwartz and Coppersmith (1984) and Sibson (1992) suggest that stress drops of ≈10 MPa are consistent with recurring quakes of M5/6 on the order of 1000 yrs in some areas. Note that the smaller events (including fault creep events and earth quake swarm events) will generate a large frequency of small pulses, which can contribute a significant volume over an extended time period. Sibson (1996) suggests that differential stresses of ≈40 MPa are probably a maxima for the operation of fault meshes or networks as enhanced flow zones. The lower range of fluid pressure pulse values (up to 10 MPa) has been used for the numerical modelling of pulsed flow across inactive fault zones presented later.

Bruhn *et al.* (1990) have calculated the approximate time needed to seal up a fracture by quartz precipitation. The model used is based upon evaluating the impact of pressure or temperature drops or saturation levels; for a pressure reduction of ≈100 MPa (equivalent to a 70°C temperature reduction) sealing times for a fracture at ≈300°C are approximately 1–100 yrs for fractures of width 0.01–1 mm. The calculation assumes that there is a reservoir of supersaturated solution and rapid fluid flow through the fracture. The estimates form a platform for calculating the sealing time on faults with different pore sizes and indicate that modelling fault zones as open systems for periods of up to a few months is appropriate. This is the period when after-shock activity following large (>M5) earthquakes is also considered to maintain an open system in the fault damage zone structure (Knipe, 1992).

THE STATISTICAL DISTRIBUTION OF POPULATION OF PULSE SIZES OVER AN EXTENDED TIME PERIOD

The number of pressure pulses which take place in a volume undergoing active faulting is indicated by the data available on seismicity activity. Note that 700,000 shocks were recorded in the 1965–1967 Matsushiro earthquake swarm (Hagiwara and Iwata, 1968). The exact distribution of events can be considered approximately fractal or power-law and earthquakes of M5/6 can take place on the order of every 1000 yrs in some tectonic areas (Scholz, 1989; Sibson, 1989).

Flow model and governing equations

DEVELOPING A FLOW MODEL

Consider a sealed fault zone behind which a hydrocarbon reservoir has accumulated and which has the potential to leak when the pressure within the hydrocarbon is raised by a transmitted pressure pulse from a nearby geological event.

The reservoir is constrained from above by a sealing cap rock and around the sides by sealing inactive faults. The hydrocarbon is supported from below by a denser water reservoir. In the initial state, the hydrocarbon remains

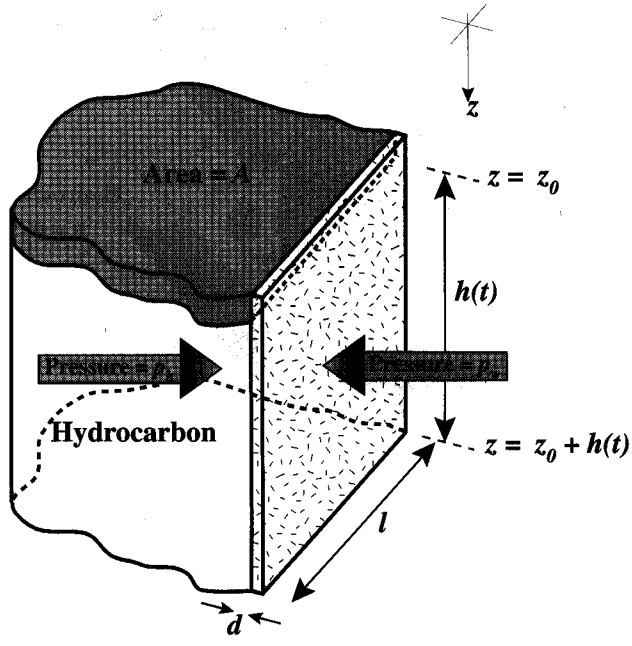

Fig. 1. *A hydrocarbon column constrained by inactive faults and a sealing cap rock.*

contained and the excess pressure within is insufficient to cause any leakage. A portion of the faulted walls bounding the hydrocarbon is then forced to cause migration of the hydrocarbon as an applied pressure pulse transmitted through the reservoir increases the pressure over some of the surface sufficiently to raise the cross-fault pressure difference above the critical pressure for the fault rock. The water reservoir bounding the base of the reservoir is assumed to extend below the lowest part of the leaking fault and along the other face of this fault so that the pressure difference across the fault, which will aid in the seepage of hydrocarbon, will be due to the difference in the densities of the water and hydrocarbon alone.

The mathematical model for the process described above is depicted in Fig. 1. The hydrocarbon reservoir is assumed to have a uniform horizontal cross section of area A. The vertical sides of the column are initially of height h_0. As flow takes place across the fault during the influence of the pressure pulse, a decrease in the hydrocarbon column height and a decrease in the undisturbed hydrocarbon pressure driving the fluid flow will occur. Here, it is assumed that no increase in the level of hydrocarbon in the reservoir can be achieved by migration into that region from other hydrocarbon reservoirs. The column height at the time t, relative to the reference time $t = 0$ at which the pressure pulse begins to act at the hydrocarbon-rock-water boundary, is then denoted by $h(t)$. Measuring the depth z vertically down through the system, let z_0 represent the constant position of the top of the column, i.e. the base of the sealing cap rock. The surface of the column side over which there is the potential for hydrocarbon migration is taken to have horizontal length l and can be assumed to

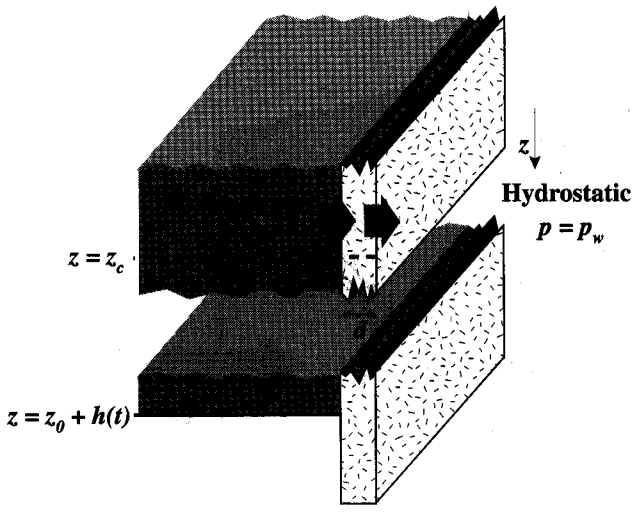

Fig. 2. *A section through the hydrocarbon-rock-water boundaries.*

be planar without significant loss of generality due to the minimal variations of quantities in the horizontal direction compared to the vertical direction. The pressure gradient which drives the flow of hydrocarbon acts over the constant distance d between the two faces of the fault rock.

A close-up of the hydrocarbon-rock-water interfaces is shown in Fig. 2. On the right-hand side of the fault rock water exists at all depths within the vicinity of the reservoir. On the other side, water exists beyond $z = z_0 + h(t)$ and hydrocarbon for $z_0 \leq z \leq (z_0 + h(t))$. Thus, if ρ_w and ρ_h denote the density of water and hydrocarbon, respectively, we have within the region of interest that

$$\begin{aligned} \rho(z) &= \rho_h, \quad z_0 \leq z \leq z_0 + h(t) \\ \rho(z) &= \rho_w, \quad z > z_0 + h(t) \end{aligned} \tag{1}$$

Relative to the reference pressure depth $z = (z_0 + h(t))$ of the hydrocarbon-water interface where $p = p_0$, the pressure within the hydrocarbon column at depth z when no pressure pulse acts is

$$p_h(z) = p_0 - \rho_h g(z_0 + h(t) - z) \tag{2}$$

and the pressure within the water on the other side of the fault is

$$p_w(z) = p_0 - \rho_w g(z_0 + h(t) - z) \tag{3}$$

where g is the acceleration due to gravity. Thus, the effect of buoyancy forces is to produce a resultant pressure at depths $z_0 \leq z < (z_0 + h(t))$ within the column as an excess to that achieved by hydrostatic pressure.

A critical entry pressure value, p_c, is introduced; this is dependent upon the permeability of the fault rock and represents the pressure difference across the inactive fault plane which must be exceeded before fluid can flow. For a given value of p_c, the hydrocarbon reservoir will remain sealed by the fault only if the ambient pressure at the top of the hydrocarbon column $z = z_0$ does not exceed the sum of hydrostatic pressure (ambient pressure on the other side of the fault plane) and the critical pressure. Thus,

$$p_h(z_0) \leq p_w(z_0) + p_c \tag{4}$$

is required for the reservoir to remain sealed by the fault. The condition (4) can be applied at $t = 0$ to impose a maximum initial hydrocarbon column height h_{max} which can be supported by the fault rock, namely

$$h_0 \leq h_{max} = \frac{p_c}{(\rho_w - \rho_h)g} \tag{5}$$

A pulse of pressure, applied to the reservoir at the reference time $t = 0$, causes an effective increase in the pressure difference across the two sides of the fault. The function describing the increase in pressure within the hydrocarbon at time t is $f(t)$. This pressure pulse function is assumed to act for a period T and reach a peak value p_d over $0 \leq t \leq T$. At any particular time throughout the period of the pulse three possible flow regimes may exist:

(i) Complete flow through the fault plane:
The value of the pressure pulse at time t is sufficient to cause flow over the depth interval $z_0 \leq z \leq (z_0 + h(t))$. Thus, complete flow exists at time t if the pressure difference across the fault at $z = z_0 + h(t)$ exceeds p_c, i.e.

$$f(t) \geq p_c \tag{6}$$

(ii) No flow over the fault plane:
The value of the pressure pulse at time t is insufficient to cause flow at the top of the reservoir $z = z_0$. Thus, no flow exists over the fault plane if

$$p_h(z_0) + f(t) \leq p_w(z_0) + p_c \tag{7}$$

This condition requires that

$$f(t) \leq p_c - (\rho_w - \rho_h)gh(t) \tag{8}$$

(iii) Partial flow over the fault plane:
The value of the pressure pulse at time t is sufficient to cause flow, but only over the reduced depth interval $z_0 \leq z \leq z_c(t)$, where $z_c(t)$ denotes the critical depth value at which flow stops at time t. Partial flow over the fault plane, therefore, requires that

$$p_c - (\rho_w - \rho_h)gh(t) < f(t) < p_c \tag{9}$$

In such cases, the flow takes place over $z_0 \leq z \leq z_c$ and z_c satisfies

$$p_h(z_c) + f(t) = p_w(z_c) + p_c \tag{10}$$

so that

$$z_c(t) = z_0 + h(t) - \frac{p_c - f(t)}{(\rho_w - \rho_h)g} \tag{11}$$

The above three conditions are represented diagrammatically in Fig. 3. The line along which $p = p_w + p_c$ shows the pressure which must be attained at any depth

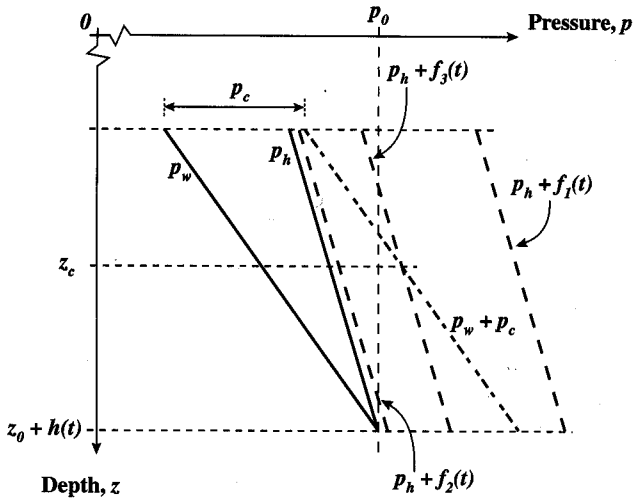

Fig. 3. *A diagram of the three possible flow regimes.*

within the hydrocarbon column for flow to commence at that point. The three values of the pressure pulse function $f(t) = f_1(t)$, $f_2(t)$ and $f_3(t)$ represent the three flow regimes (i)–(iii), respectively, listed above.

If the pressure pulse function is continuous over the time interval $[0, T]$, the flow across the fault plane may evolve in three distinct ways, depending upon the peak value of the pulse p_d:

(i) No flow at all times:
The pulse is insufficient to cause flow at any time $t \in [0, T]$ and hence

$$p_d \leq p_c - (\rho_w - \rho_h)gh_0 \tag{12}$$

from equation (8).

(ii) No flow initially, followed by partial flow, and a return to no flow:
Flow begins at $z = z_0$ at some time $t_1^{z_0}$ within the period of the pressure pulse, but the peak pressure p_d is insufficient to achieve complete flow. Thus,

$$p_c - (\rho_w - \rho_h)gh_0 < p_d < p_c \tag{13}$$

and the value of $t_1^{z_0}$ is deduced by solving the following equation:

$$f(t_1^{z_0}) = p_c - (\rho_w - \rho_h)gh_0 \tag{14}$$

At a second time $t_2^{z_0} \in [0, T]$ flow across the fault ceases. This time is implicitly defined by the following relationship:

$$f(t_2^{z_0}) = p_c - (\rho_w - \rho_h)gh(t_2^{z_0}) \tag{15}$$

(iii) No flow initially, followed by partial flow, complete flow, partial flow and no flow:
Complete flow is achieved over a time interval from $t = t_1^c$ to $t = t_2^c$, the limits of this period corresponding to the times at which the complete flow condition (6) is satisfied. This requires that the peak pulse pressure be at least p_c. Thus, there is no flow for $t \in [0, t_1^{z_0})$; partial flow for $t \in [t_1^{z_0}, t_1^c)$; complete flow for $t \in [t_1^c, t_2^c]$; a return to partial flow for $t \in (t_2^c, t_2^{z_0}]$; no flow for $t \in (t_2^{z_0}, T]$.

If the pressure pulse function is discontinuous over the time interval $[0, T]$, flow may start instantaneously or stop over the whole fault plane without the intermediate stage of partial flow.

DERIVATION OF THE GOVERNING EQUATIONS

If d (the fault thickness) is small, the velocity of the fluid flowing through the fault plane at the depth z when the pressure difference is large enough can be assumed to be independent of x, the horizontal coordinate perpendicular to the plane of the fault, and, assuming that the flow satisfies Darcy's law, can be approximated by the relation

$$v(z, t) = -\frac{K}{\mu}\frac{\partial p}{\partial x} \approx -\frac{K}{\mu}\frac{\Delta p(z, t)}{d} \tag{16}$$

where K is the permeability of the rock, μ is molecular viscosity and $\Delta p(z, t)$ denotes the pressure difference over and above the critical entry pressure at the depth z due to the pulse at time t:

$$\begin{aligned}\Delta p(z, t) &= p_w(z) + p_c - p_h(z) - f(t) \\ &= p_c - (\rho_w - \rho_h)g(z_0 + h(t) - z) - f(t)\end{aligned} \tag{17}$$

Suppose now that flow takes place at depth z for some small time interval δt across an elemental portion of the fault plane of width δz and horizontal length l (the extent of the hydrocarbon reservoir across the fault plane). The small volume of fluid migrating across the fault plane in this time interval is $\delta V(z, t)$. Thus,

$$\begin{aligned}\delta V(z, t) &= l\delta t \int_z^{z+\delta z} v(z', t)\, dz' \\ &= \frac{\delta z \delta t K l}{\mu d}[(\rho_w - \rho_h)g(z_0 + h(t) - z) \\ &\quad + f(t) - p_c]\end{aligned} \tag{18}$$

and the volume flow rate across the elemental volume of width δz is

$$\begin{aligned}\frac{dV}{dt}(z, t) &= \frac{\delta z K l}{\mu d}[(\rho_w - \rho_h)g(z_0 + h(t) - z) \\ &\quad + f(t) - p_c]\end{aligned} \tag{19}$$

The flow rate over the whole fault plane at time t depends upon the value of the pressure pulse and whether there is no flow, partial flow or complete flow. The equations governing the fluid flow rate and, hence the height of the hydrocarbon column, must be derived separately depending on whether the flow is over part or all of the fault plane:

(i) Partial flow over the fault plane:
The value of the pressure pulse function $f(t)$ satisfies

condition (9) and flow occurs over a limited range of depths $z_0 \leq z \leq z_c$, where z_c is defined in equation (11), within the fault plane. The total volume flow rate over the surface of the fault at time t when partial flow occurs is defined by

$$\frac{d\tilde{V}}{dt}(t) = \int_{z_0}^{z_c} \frac{Kl}{\mu d}[(\rho_w - \rho_h)g(z_0 + h(t) - z) + f(t) - p_c]\,dz \quad (20)$$

using equation (19). The volume of hydrocarbon, $\tilde{V}$, which has migrated across the fault plane can be expressed as the horizontal surface area of the reservoir multiplied by the loss in height of the column, i.e.

$$\text{Total volume migration} = \tilde{V}(t) = A(h_0 - h(t)) \quad (21)$$

and, hence, the equation governing the height of the hydrocarbon column when partial flow is occurring is given by

$$\frac{dh}{dt}(t) = -\frac{1}{A}\frac{d\tilde{V}}{dt}(t) = -\frac{Kl}{2\mu Ad(\rho_w - \rho_h)g}[(\rho_w - \rho_h)gh(t) + f(t) - p_c]^2 \quad (22)$$

(ii) Complete flow over the fault plane:
The value of the pressure pulse function $f(t)$ satisfies condition (6) and flow occurs over the complete range of depths $z_0 \leq z \leq (z_0 + h(t))$. Using equation (19), the total volume flow rate over the surface of the fault at time t when complete flow occurs is defined by

$$\frac{d\tilde{V}}{dt}(t) = \int_{z_0}^{z_0+h(t)} \frac{Kl}{\mu d}[(\rho_w - \rho_h)g(z_0 + h(t) - z) + f(t) - p_c]\,dz \quad (23)$$

and, hence, the equation governing the height of the hydrocarbon column when complete flow is occurring is given by

$$\frac{dh}{dt}(t) = -\frac{Kl}{\mu Ad}\left[\frac{1}{2}(\rho_w - \rho_h)gh(t) + f(t) - p_c\right]h(t) \quad (24)$$

NON-DIMENSIONALISATION OF THE GOVERNING EQUATIONS

To obtain a non-dimensional version of each of the governing equations (22), defining partial flow over the fault plane, and (24), defining complete flow over the fault plane, non-dimensional variables τ, s, $H(\tau)$ are defined as

$$\tau = \frac{t}{T}, \quad s = \frac{z - z_0}{h_0}, \quad H = \frac{h}{h_0} \quad (25)$$

the non-dimensional function $F(\tau)$ is defined by

$$F = \frac{f}{\rho_w g h_0} \quad (26)$$

and the following non-dimensional parameters are introduced:

$$p_c^* = \frac{p_c}{\rho_w g h_0}, \quad p_d^* = \frac{p_d}{\rho_w g h_0}, \quad \beta = \frac{KlT\rho_w g h_0}{\mu Ad} \quad (27)$$

where p_c^* is the non-dimensional critical pressure and p_d^* is the non-dimensional peak value of the pressure pulse function.

As a result of this non-dimensionalisation, the flow characteristics can be summarised as follows:
If $H_{max} = \frac{h_{max}}{h_0}$ denotes the non-dimensional initial hydrocarbon column height which can be supported by the fault rock, equation (5) requires that

$$1 \leq H_{max} = \frac{p_c^*}{1 - \frac{\rho_h}{\rho_w}} \quad (28)$$

and, thus, the following restriction may be imposed upon the value of the parameter p_c^*:

$$p_c^* \geq 1 - \frac{\rho_h}{\rho_w} \quad (29)$$

(i) Partial flow over the fault plane:
The value of the non-dimensional pressure pulse function $F(\tau)$ satisfies

$$p_c^* - \left(1 - \frac{\rho_h}{\rho_w}\right)H(\tau) < F(\tau) < p_c^* \quad (30)$$

and flow occurs over a limited range of non-dimensional depths $0 \leq s \leq s_c(\tau)$, where $s_c(\tau)$ is the critical non-dimensional depth at which flow stops and is defined by

$$s_c(\tau) = H(\tau) - \frac{p_c^* - F(\tau)}{1 - \frac{\rho_h}{\rho_w}} \quad (31)$$

The equation governing the height of the hydrocarbon column when partial flow is occurring is given by

$$\frac{dH}{d\tau}(\tau) = -\frac{\beta}{2\left(1 - \frac{\rho_h}{\rho_w}\right)}\left[\left(1 - \frac{\rho_h}{\rho_w}\right)H + F - p_c^*\right]^2 \quad (32)$$

It is also clear from equations (30)–(32) that if partial flow is achieved without progressing to complete flow through the period of the pulse, i.e.

$$p_c^* - \left(1 - \frac{\rho_h}{\rho_w}\right)H(\tau) < p_d^* < p_c^* \quad (33)$$

then the non-dimensional height of the hydrocarbon column must approach a limiting value

$$H \to \frac{p_c^* - p_d^*}{1 - \frac{\rho_h}{\rho_w}} \quad (34)$$

for any value of the parameter β, i.e. for any period of pulse, and for any form of the function $F(\tau)$. This result shows that the hydrocarbon column can never be exhausted if the maximum of the pressure pulse function has a magnitude less than the critical pressure.

(ii) Complete flow over the fault plane:
The value of the non-dimensional pressure pulse function $F(\tau)$ satisfies

$$F(\tau) \geq p_c^* \tag{35}$$

and flow occurs over the complete range of non-dimensional depths $0 \leq s \leq H(\tau)$. The equation governing the height of the hydrocarbon column when complete flow is occurring is given by

$$\frac{dH}{d\tau}(\tau) = -\beta\left[\frac{1}{2}\left(1 - \frac{\rho_h}{\rho_w}\right)H + F - p_c^*\right]H \tag{36}$$

SOLUTION OF THE GOVERNING EQUATIONS

For a given pressure pulse function, the problem reduces to the solution of at least one first-order differential equation. At times when partial flow is occurring, the height of the hydrocarbon column is governed by equation (32) and, at times when complete flow over the fault plane occurs, the governing evolution is given by equation (36). The solution of these nonlinear differential equations is now discussed separately, beginning with the equation governing complete flow:

(i) Equation (36) governing complete flow
The non-dimensional height of the hydrocarbon column when complete flow is occurring is governed by the Bernoulli equation

$$H' - [\beta(p_c^* - F(\tau))]H = \left[-\frac{\beta}{2}\left(1 - \frac{\rho_h}{\rho_w}\right)\right]H^2 \tag{37}$$

where prime denotes differentiation with respect to time τ. Equation (37) can be reduced to a linear equation by the change of variable $r = \frac{1}{H}$. The function $r(\tau)$ then satisfies

$$r' + [\beta(p_c^* - F(\tau))]r = \frac{\beta}{2}\left(1 - \frac{\rho_h}{\rho_w}\right) \tag{38}$$

The general solution of this linear equation can be obtained readily as

$$r(\tau) = e^{-\beta(p_c^*\tau - \int^\tau F(\tilde{\tau})\,d\tilde{\tau})} \times \left[C + \frac{\beta}{2}\left(1 - \frac{\rho_h}{\rho_w}\right)\int^\tau e^{\beta\left(p_c^*\tau' - \int^{\tau'} F(\tilde{\tau})\,d\tilde{\tau}\right)}\,d\tau'\right] \tag{39}$$

for some constant of integration C. In general, the governing equation (37) for complete flow may be valid over some non-dimensional time interval $\tau_1^c \leq \tau \leq \tau_2^c$ with an initial non-dimensional hydrocarbon column height specified, namely $H(\tau_1^c) = H_0^c$. Applying this initial condition, the following expression for $H(\tau)$ can be recovered:

$$H(\tau) = e^{\mathcal{F}(\tau)}\left[\frac{1}{H_0^c}e^{\mathcal{F}(\tau_1^c)} + \frac{\beta}{2}\left(1 - \frac{\rho_h}{\rho_w}\right)\int_{\tau_1^c}^\tau e^{\mathcal{F}(\tau')}\,d\tau'\right]^{-1} \tag{40}$$

where the function

$$\mathcal{F}(\tau) = \beta\left(p_c^*\tau - \int^\tau F(\tilde{\tau})\,d\tilde{\tau}\right) \tag{41}$$

has been introduced. The value of H at the end of the non-dimensional time interval, τ_2^c, may then be predicted using equation (40).

(ii) Equation (32) governing partial flow
The non-dimensional height of the hydrocarbon column when partial flow is occurring is governed by equation (32). In general, this equation cannot be solved by elementary methods. However, if a particular solution $H_1(t)$ is known then the general solution has the form

$$H(\tau) = H_1(\tau) + \tilde{H}(\tau) \tag{42}$$

where $\tilde{H}(\tau)$ is the general solution of the Bernoulli equation

$$\tilde{H}' - \beta\left[p_c^* - F(\tau) - \left(1 - \frac{\rho_h}{\rho_w}\right)H_1(\tau)\right]\tilde{H} = \left[-\frac{\beta}{2}\left(1 - \frac{\rho_h}{\rho_w}\right)\right]\tilde{H}^2 \tag{43}$$

This Bernoulli equation can be solved using the change of variable which was applied to equation (37) above. The governing equation (32) for partial flow may be valid over some non-dimensional time interval $\tau_1^p \leq \tau \leq \tau_2^p$ with an initial hydrocarbon column height specified, namely $H(\tau_1^p) = H_0^p$. Thus, the required particular solution of the Bernoulli equation (43) follows by applying the initial condition

$$\tilde{H}(\tau_1^p) = H_0^p - H_1(\tau_1^p) \tag{44}$$

and is given explicitly as

$$\tilde{H}(\tau) = e^{\tilde{\mathcal{F}}(\tau)}\left[\frac{1}{H_0^p - H_1(\tau_1^p)}e^{\tilde{\mathcal{F}}(\tau_1^p)} + \frac{\beta}{2}\left(1 - \frac{\rho_h}{\rho_w}\right)\int_{\tau_1^p}^\tau e^{\tilde{\mathcal{F}}(\tau')}\,d\tau'\right]^{-1} \tag{45}$$

where

$$\tilde{\mathcal{F}}(\tau) = \beta\left[p_c^*\tau - \int^\tau \left(F(\tilde{\tau}) + \left(1 - \frac{\rho_h}{\rho_w}\right)H_1(\tilde{\tau})\right)d\tilde{\tau}\right] \tag{46}$$

THE EFFECTIVE IMPULSE IMPARTED TO THE FLUID

The variation of the decrease in non-dimensional hydrocarbon column height with the non-dimensional parameters β, p_c^* and p_d^* can be characterised from an alternative perspective by introducing the quantities

$$I_p = \int_{\mathcal{T}_p}\int_0^{s_c(\tau)} p_{eff}\,ds\,d\tau \tag{47}$$

for the total time interval $\mathcal{T}_p$ when partial flow is occurring and

$$I_c = \int_{\mathcal{T}_c} \int_0^{H(\tau)} p_{eff}\, ds\, d\tau \tag{48}$$

for the total time interval $\mathcal{T}_c$ when complete flow is occurring. $(I_c + I_p)$ is considered to be the effective impulse imparted to the hydrocarbon over the duration of the pressure pulse so as to cause migration over the fault plane. The notation p_{eff} is used to indicate integration of the effective pressure difference at any non-dimensional depth s and time τ only when flow is occurring. This effective pressure difference is defined to be

$$p_{eff} = F(\tau) + \left(1 - \frac{\rho_h}{\rho_w}\right)(H(\tau) - s) - p_c^* \tag{49}$$

where the second term is the buoyancy pressure at depth s and time τ due to the hydrocarbon column of height $(H(\tau) - s)$ which lies *below* the depth s. Direct integration of equations (47) and (48) with respect to s leads to

$$I_p = \frac{1}{2}\left(1 - \frac{\rho_h}{\rho_w}\right) \int_{\mathcal{T}_p} s_c^2\, d\tau \tag{50}$$

and

$$I_c = \int_{\mathcal{T}_c} \left[\frac{1}{2}\left(1 - \frac{\rho_h}{\rho_w}\right) H + F - p_c^*\right] H\, d\tau \tag{51}$$

The governing ordinary differential equations (32) and (36) for partial and complete flow, respectively, can be used to directly relate these effective impulses to losses in hydrocarbon column height as follows:

$$I_p = -\frac{1}{\beta}[H(\tau)]_{\mathcal{T}_p}, \quad I_c = -\frac{1}{\beta}[H(\tau)]_{\mathcal{T}_c} \tag{52}$$

where the notation $[H(\tau)]_{\mathcal{T}}$ denotes the total change in $H(\tau)$ over the time period $\mathcal{T}$. Thus, the total effective impulse imparted to the hydrocarbon over the period $\mathcal{T} \subseteq [0, 1]$ for which flow over the fault plane takes place is

$$I = I_p + I_c = \frac{1}{\beta}(1 - H(1)) \tag{53}$$

and I is directly proportional to the decrease in hydrocarbon column height due to the pressure pulse.

Application to specific pressure pulse functions

In this section, the general discussion presented earlier is applied to some particular functions defining the pressure pulse. In the first example, the non-dimensional pressure pulse is assumed to take the form of a discontinuous step function with value p_d^* and the governing equations can be solved analytically. In the second example, the non-dimensional pressure pulse reflects a linear increase from zero to the peak p_d^* at the non-dimensional time $\tau = \tau_p$, followed by a linear decrease down to zero again at the non-dimensional time $\tau = 1$, the non-dimensional period of the pulse. The majority of the first-order governing equations in this section are solved analytically before a transfer to numerical techniques is suggested for applications to more complex pressure pulse functions. The analytical results presented in this section will be displayed graphically for some appropriate ranges of the non-dimensional parameters β, p_d^* and p_c^*.

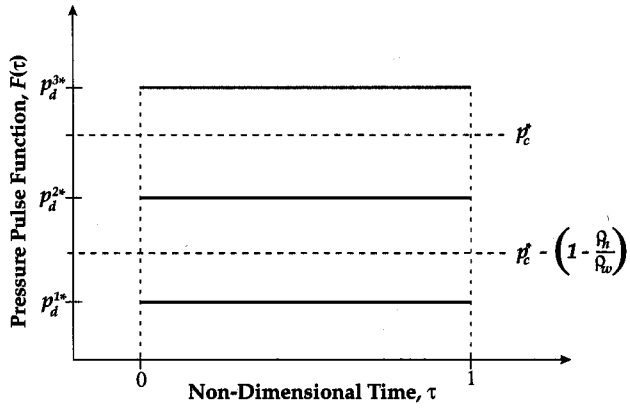

Fig. 4. *The flow regimes associated with different values of the non-dimensional step pressure pulse function.*

EXAMPLE: *the step pressure pulse function*

At the reference time $\tau = 0$, the non-dimensional pressure pulse function describes an instantaneous increase by an amount p_d^* and this value persists until $\tau = 1$, as shown in Fig. 4. The value of p_d^* critically determines whether flow occurs and, if it does, whether flow occurs over the whole depth of the hydrocarbon reservoir or only partially over the reservoir. The three different flow regimes are depicted in Fig. 4 by three suitable step functions with non-dimensional pressure values p_d^{1*}, p_d^{2*} and p_d^{3*} described as follows:

(i) No flow:
The non-dimensional pressure pulse function is a step function with value p_d^{1*} and the associated non-dimensional pressure increase is insufficient to cause flow at the top of the reservoir. Hence

$$p_d^{1*} \leq p_c^* - \left(1 - \frac{\rho_h}{\rho_w}\right) \tag{54}$$

using equation (12).

(ii) Partial flow over the fault plane:
At time $\tau = 0$, a non-dimensional pressure pulse step function with value p_d^{2*} initiates flow over the fault plane. However, the magnitude of the pulse function is insufficient to cause flow at all depths over the height of the hydrocarbon column and flow instantaneously begins over only a limited range of non-dimensional depths $0 \leq s \leq s_c(\tau)$,

where $s_c(\tau)$ is defined in equation (31). Hence,

$$p_c^* - \left(1 - \frac{\rho_h}{\rho_w}\right) < p_d^{2*} < p_c^* \tag{55}$$

and the largest non-dimensional depth at which flow occurs at non-dimensional time τ is

$$s_c(\tau) = H(\tau) - \frac{p_c^* - p_d^{2*}}{\left(1 - \frac{\rho_h}{\rho_w}\right)} \tag{56}$$

Following the analysis presented earlier, the non-dimensional time τ_1^p becomes $\tau_1^p = 0$. The equation governing the height of the hydrocarbon column at non-dimensional time τ is given by

$$H' = -\frac{\beta}{2\left(1 - \frac{\rho_h}{\rho_w}\right)}\left[\left(1 - \frac{\rho_h}{\rho_w}\right)H + p_d^{2*} - p_c^*\right]^2 \tag{57}$$

subject to the initial condition

$$H(\tau_1^p) = H(0) = 1 \tag{58}$$

The evolution of the non-dimensional hydrocarbon column height $H(\tau)$ can be obtained by a simple integration in this case. However, this example is used to illustrate the general approach given earlier. The differential equation (57) possesses the particular solution

$$H_1(\tau) = \frac{p_c^* - p_d^{2*}}{1 - \frac{\rho_h}{\rho_w}} \tag{59}$$

and hence the general solution (42) can be derived by solving the Bernoulli equation (43) for $\tilde{H}(\tau)$, given explicitly in this example by the differential equation

$$\tilde{H}' = -\frac{\beta}{2}\left(1 - \frac{\rho_h}{\rho_w}\right)\tilde{H}^2 \tag{60}$$

Solving equation (60) subject to the initial condition

$$\tilde{H}(0) = 1 - H_1(0) = 1 - \frac{p_c^* - p_d^{2*}}{1 - \frac{\rho_h}{\rho_w}} \tag{61}$$

either directly or by substitution into the particular solution (45), gives

$$\tilde{H}(\tau) = \frac{1}{\left(1 - \frac{\rho_h}{\rho_w}\right)}\left[\frac{\beta}{2}\tau + \frac{1}{1 - \frac{\rho_h}{\rho_w} - p_c^* + p_d^{2*}}\right]^{-1} \tag{62}$$

and therefore the variation in non-dimensional height of the hydrocarbon column evolves according to

$$H(\tau) = \frac{1}{\left(1 - \frac{\rho_h}{\rho_w}\right)} \times \left\{\left[\frac{\beta}{2}\tau + \frac{1}{1 - \frac{\rho_h}{\rho_w} - p_c^* + p_d^{2*}}\right]^{-1} + p_c^* - p_d^{2*}\right\} \tag{63}$$

At time τ, the largest non-dimensional depth at which flow occurs is given by equation (56) as

$$s_c(\tau) = \frac{1}{\left(1 - \frac{\rho_h}{\rho_w}\right)}\left[\frac{\beta}{2}\tau + \frac{1}{1 - \frac{\rho_h}{\rho_w} - p_c^* + p_d^{2*}}\right]^{-1} \tag{64}$$

The influence of the pressure pulse ceases at $\tau = 1$, the final non-dimensional height of the hydrocarbon column at this time being

$$H(1) = \frac{1}{\left(1 - \frac{\rho_h}{\rho_w}\right)} \times \left\{\left[\frac{\beta}{2} + \frac{1}{1 - \frac{\rho_h}{\rho_w} - p_c^* + p_d^{2*}}\right]^{-1} + p_c^* - p_d^{2*}\right\} \tag{65}$$

Equation (64) also predicts the largest non-dimensional depth at which hydrocarbon migrates across the fault just before the pressure pulse ceases. It becomes clear from the value of $s_c(1)$ that flow can stop before the non-dimensional pressure pulse period $\tau = 1$ only in the limiting case $\beta \to \infty$, corresponding to $T \to \infty$. Thus, for a pulse of finite period, partial flow over the fault plane continues throughout the period of the pulse. Furthermore, the hydrocarbon column can never be exhausted since the limiting, infinite period, case $\beta \to \infty$, requires that $H(1)$ also approaches a limiting value:

$$H(1) \to \frac{p_c^* - p_d^{2*}}{\left(1 - \frac{\rho_h}{\rho_w}\right)} \quad \text{as } \beta \to \infty,\ T \to \infty \tag{66}$$

as stated for the general non-dimensional pressure pulse function $F(\tau)$ in equation (34).

From condition (55), it can be shown that

$$0 < p_d^{2*} - p_c^* + \left(1 - \frac{\rho_h}{\rho_w}\right) < \left(1 - \frac{\rho_h}{\rho_w}\right) \tag{67}$$

so that the term $\beta\left(p_d^{2*} - p_c^* + \left(1 - \frac{\rho_h}{\rho_w}\right)\right)\tau$ can be considered to be small provided that $\beta < 1$. In this case, the solution (63) can be expanded to give the approximate linear evolution for $H(\tau)$ as

$$H(\tau) \approx 1 - \frac{1}{2}\frac{\beta}{\left(1 - \frac{\rho_h}{\rho_w}\right)}\left(p_d^{2*} - p_c^* + \left(1 - \frac{\rho_h}{\rho_w}\right)\right)^2\tau \tag{68}$$

(iii) Complete flow over the fault plane:

At non-dimensional time $\tau = 0$ a non-dimensional pressure pulse step function with value p_d^{3*} initiates flow over the fault plane. The magnitude of the pulse function is sufficient to cause flow at all depths over the height of the hydrocarbon column. Hence,

$$p_d^{3*} \geq p_c^* \tag{69}$$

and, following the analysis earlier, $\tau_1^c = 0$. The equation governing the height of the hydrocarbon column at time τ is given by

$$H' + [\beta(p_d^{3*} - p_c^*)]H = \left[-\frac{\beta}{2}\left(1 - \frac{\rho_h}{\rho_w}\right)\right] H^2 \quad (70)$$

subject to the initial condition

$$H(\tau_1^c) = H(0) = 1 \quad (71)$$

Solving the differential equation (70) either directly or by substitution into the particular solution (40), the height of the hydrocarbon column evolves according to

$$H(\tau) = \left\{\left[1 + \frac{1}{2}\left(\frac{1 - \frac{\rho_h}{\rho_w}}{p_d^{3*} - p_c^*}\right)\right] e^{\beta(p_d^{3*} - p_c^*)\tau} - \frac{1}{2}\left(\frac{1 - \frac{\rho_h}{\rho_w}}{p_d^{3*} - p_c^*}\right)\right\}^{-1} \quad (72)$$

The influence of the pressure pulse ceases at $\tau = 1$, the final height of the hydrocarbon column being defined by equation (72). In the limiting case $\beta \to \infty$, corresponding to $T \to \infty$, $H(1) \to 0$. Thus, if the pressure pulse is of sufficient magnitude to cause complete flow over the fault plane, the hydrocarbon column could be exhausted in the limiting, infinite period, case. This result is in contrast to the situation when only partial flow is present over the fault plane; it was shown that the final non-dimensional hydrocarbon column height approached a limiting value as the period of the pulse was increased.

The evolution of the hydrocarbon column height can also be investigated for the cases in which $\beta(p_d^{3*} - p_c^*) \ll 1$. By expanding the expression (72) in powers of this small parameter, it can be shown that

$$H(\tau) = 1 - \beta\left[p_d^{3*} - p_c^* + \frac{1}{2}\left(1 - \frac{\rho_h}{\rho_w}\right)\right]\tau + \mathbf{O}((\beta(p_d^{3*} - p_c^*))^2) \quad (73)$$

Thus, if $\beta(p_d^{3*} - p_c^*) \ll 1$, the evolution of $H(\tau)$ is approximately linear with non-dimensional time τ.

The solutions (63) and (72) must be continuous with respect to the value of the step function when the step function has the value p_c^*. This can be confirmed, since as $p_d^{2*} \to p_c^*$ in equation (63) for the evolution of $H(\tau)$ under partial flow conditions and as $p_d^{3*} \to p_c^*$ in equation (72) for the evolution of $H(\tau)$ under complete flow conditions, both solutions approach the limiting function

$$H(\tau) = \left[1 + \frac{\beta}{2}\left(1 - \frac{\rho_h}{\rho_w}\right)\tau\right]^{-1} \quad (74)$$

EXAMPLE: *the linear pressure pulse function*

Over the time interval $0 \le \tau \le \tau_p$ the non-dimensional pressure pulse function describes a linear increase in non-dimensional pressure, the peak value of pressure p_d^* then being achieved at $\tau = \tau_p$. A linear decrease in the pressure pulse function then follows until $\tau = 1$ when the pressure returns to ambient, as shown in Fig. 5. The three different flow regimes are depicted in Fig. 5 by three suitable linear functions having non-dimensional peak pressure values p_d^{1*}, p_d^{2*} and p_d^{3*} described as follows:

(i) No flow:
The pressure pulse function is insufficient to cause flow at the top of the reservoir. Hence, condition (54) is satisfied.

(ii) Partial flow over the fault plane:
At non-dimensional time $\tau = 0$ the non-dimensional pressure pulse function

$$F(\tau) = \begin{cases} p_d^{2*}\dfrac{\tau}{\tau_p}, & \text{for } 0 \le \tau \le \tau_p \\ p_d^{2*}\dfrac{1-\tau}{1-\tau_p}, & \text{for } \tau_p \le \tau \le 1 \end{cases} \quad (75)$$

with peak value p_d^{2*} initiates a pressure increase within the hydrocarbon column. The initial pressure increase is insufficient to start flow over the fault plane until the time τ_1^p is reached. Beyond the time τ_1^p partial flow exists over the fault plane but the magnitude of the peak of the non-dimensional pressure pulse function is insufficient to cause flow at all depths over the height of the hydrocarbon column. Thus, the window over which hydrocarbon migrates across the fault plane decreases until at the time τ_2^p flow ceases. Hence, condition (55) is satisfied, partial flow begins at the non-dimensional time

$$\tau_1^p = \frac{\tau_p}{p_d^{2*}}\left[p_c^* - \left(1 - \frac{\rho_h}{\rho_w}\right)\right] \quad (76)$$

and ceases at the non-dimensional time τ_2^p, defined implicitly by the relation

$$p_d^{2*}\frac{1 - \tau_2^p}{1 - \tau_p} = p_c^* - \left(1 - \frac{\rho_h}{\rho_w}\right) H(\tau_2^p) \quad (77)$$

The largest depth at which flow occurs at any non-dimensional time $\tau_1^p \le \tau \le \tau_2^p$ is

$$s_c(\tau) = \begin{cases} H(\tau) - \dfrac{p_c^* - p_d^{2*}\frac{\tau}{\tau_p}}{1 - \frac{\rho_h}{\rho_w}} & \text{for } \tau_1^p \le \tau \le \tau_p \\ H(\tau) - \dfrac{p_c^* - p_d^{2*}\frac{1-\tau}{1-\tau_p}}{1 - \frac{\rho_h}{\rho_w}} & \text{for } \tau_p \le \tau \le \tau_2^p \end{cases} \quad (78)$$

Following the approach earlier, the differential equation (32) applied over the interval $\tau_1^p \le \tau \le \tau_p$ possesses the particular solution

$$H_1(\tau) = \frac{1}{1 - \frac{\rho_h}{\rho_w}}\left[p_c^* + \sqrt{\frac{2p_d^{2*}}{\beta\tau_p}} - p_d^{2*}\frac{\tau}{\tau_p}\right] \quad (79)$$

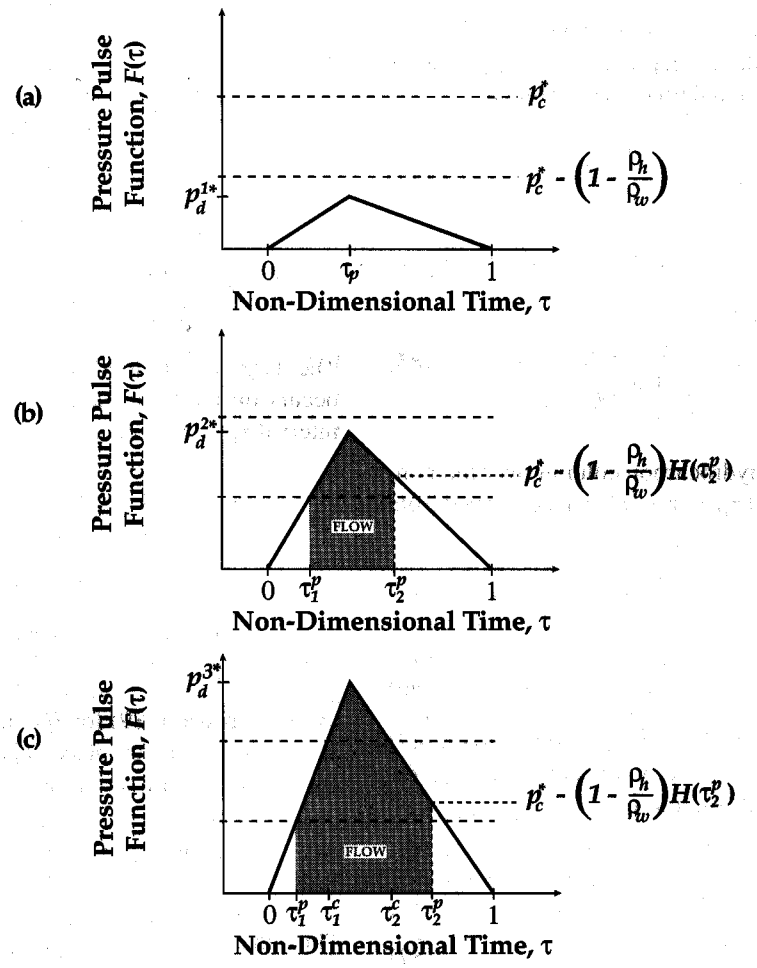

Fig. 5. *The flow regimes associated with different values of the linear non-dimensional pressure pulse function: (a) No flow; (b) Partial flow over the fault plane; (c) Complete flow over the fault plane.*

and hence the general solution (42) can be derived by solving the Bernoulli equation (43) for $\tilde{H}(\tau)$ subject to the initial condition

$$\tilde{H}(\tau_1^p) = -\frac{1}{1-\frac{\rho_h}{\rho_w}}\sqrt{\frac{2p_d^{2*}}{\beta\tau_p}} \tag{80}$$

since $H(\tau_1^p) = 1$ and τ_1^p denotes the non-dimensional time at which the magnitude of the non-dimensional pressure pulse is sufficient to initiate flow at the top of the reservoir. From the particular solution (45),

$$\tilde{H}(\tau) = -\frac{2}{1-\frac{\rho_h}{\rho_w}}\sqrt{\frac{2p_d^{2*}}{\beta\tau_p}} \times \left[1 + e^{\sqrt{\frac{2\beta\tau_p}{p_d^{2*}}}\left(p_d^{2*}\frac{\tau}{\tau_p} - p_c^* + \left(1-\frac{\rho_h}{\rho_w}\right)\right)}\right]^{-1} \tag{81}$$

and therefore the variation in non-dimensional height of the hydrocarbon column evolves according to

$$H(\tau) = \frac{1}{1-\frac{\rho_h}{\rho_w}}\left\{p_c^* - p_d^{2*}\frac{\tau}{\tau_p} + \sqrt{\frac{2p_d^{2*}}{\beta\tau_p}}\left(1 - 2\left[1 + e^{\sqrt{\frac{2\beta\tau_p}{p_d^{2*}}}\left(p_d^{2*}\frac{\tau}{\tau_p} - p_c^* + \left(1-\frac{\rho_h}{\rho_w}\right)\right)}\right]^{-1}\right)\right\} \tag{82}$$

while the largest non-dimensional depth (78) at which flow occurs over the fault plane is given explicitly as

$$s_c(\tau) = \frac{1}{1-\frac{\rho_h}{\rho_w}}\sqrt{\frac{2p_d^{2*}}{\beta\tau_p}} \times \left\{1 - 2\left[1 + e^{\sqrt{\frac{2\beta\tau_p}{p_d^{2*}}}\left(p_d^{2*}\frac{\tau}{\tau_p} - p_c^* + \left(1-\frac{\rho_h}{\rho_w}\right)\right)}\right]^{-1}\right\} \tag{83}$$

for $\tau_1^p \leq \tau \leq \tau_p$. If $\beta \ll 1$, it can be shown that the non-dimensional critical depth, $s_c(\tau)$, progresses approximately linearly with non-dimensional time τ according to

$$s_c(\tau) \approx 1 - \frac{p_c^* - p_d^{2*}\frac{\tau}{\tau_p}}{1 - \frac{\rho_h}{\rho_w}} \tag{84}$$

over the interval $\tau_1^p \leq \tau \leq \tau_p$ and reaches the maximum value

$$s_c(\tau_p) \approx 1 - \frac{p_c^* - p_d^{2*}}{1 - \frac{\rho_h}{\rho_w}} \tag{85}$$

at the time τ_p.

The evolution of the hydrocarbon column over the non-dimensional time interval $\tau_p \leq \tau \leq \tau_2^p$ can be derived from the particular solution

$$H_1(\tau) = \frac{1}{1 - \frac{\rho_h}{\rho_w}} \left[p_c^* + i\sqrt{\frac{2p_d^{2*}}{\beta(1-\tau_p)}} - p_d^{2*}\frac{1-\tau}{1-\tau_p} \right] \tag{86}$$

to the differential equation (32). The general solution (42) then follows by solving the Bernoulli equation (43) for $\tilde{H}(\tau)$ subject to the initial condition

$$\tilde{H}(\tau_p) = H_{\tau_p} - \frac{1}{1 - \frac{\rho_h}{\rho_w}} \left[p_c^* + i\sqrt{\frac{2p_d^{2*}}{\beta(1-\tau_p)}} - p_d^{2*} \right] \tag{87}$$

where H_{τ_p} denotes the evaluation of the hydrocarbon column height at the end of the time interval $\tau_1^p \leq \tau \leq \tau_p$ according to equation (82) and is given explicitly as

$$H_{\tau_p} = \frac{1}{1 - \frac{\rho_h}{\rho_w}} \left\{ p_c^* + \sqrt{\frac{2p_d^{2*}}{\beta\tau_p}} - p_d^{2*} - 2\sqrt{\frac{2p_d^{2*}}{\beta\tau_p}} \left[1 + e^{\sqrt{\frac{2\beta\tau_p}{p_d^{2*}}}\left(p_d^{2*} - p_c^* + \left(1 - \frac{\rho_h}{\rho_w}\right)\right)} \right]^{-1} \right\} \tag{88}$$

The variation in the non-dimensional height, $H(\tau)$, of the hydrocarbon column over the non-dimensional time interval $\tau_p \leq \tau \leq \tau_2^p$ can be shown to evolve according to

$$H(\tau) = \frac{1}{1 - \frac{\rho_h}{\rho_w}} \left\{ p_c^* - p_d^{2*}\frac{1-\tau}{1-\tau_p} + \sqrt{\frac{2p_d^{2*}}{\beta(1-\tau_p)}} \times \left[\frac{\Omega\cos\theta - \Gamma\sin\theta}{2\tau_p e^{-\gamma} + \frac{1}{2}\left(1 - e^{-\gamma}\right)^2 + \Omega\sin\theta + \Gamma\cos\theta} \right] \right\} \tag{89}$$

where

$$\Omega = \sqrt{\tau_p}\sqrt{1-\tau_p}(1 - e^{-2\gamma}),$$
$$\Gamma = \tau_p(1 + e^{-2\gamma}) - \tfrac{1}{2}(1 - e^{-\gamma})^2$$
$$\theta(\tau) = (\tau - \tau_p)\sqrt{\frac{2p_d^{2*}\beta}{1-\tau_p}},$$
$$\gamma = \sqrt{\frac{2\beta\tau_p}{p_d^{2*}}}\left(p_d^{2*} - p_c^* + \left(1 - \frac{\rho_h}{\rho_w}\right)\right) \tag{90}$$

The largest non-dimensional depth (78) at which flow occurs on the fault plane over the non-dimensional time interval $\tau_p \leq \tau \leq \tau_2^p$ can now be evaluated as

$$s_c(\tau) = \frac{1}{1 - \frac{\rho_h}{\rho_w}}\sqrt{\frac{2p_d^{2*}}{\beta(1-\tau_p)}} \times \left[\frac{\Omega\cos\theta - \Gamma\sin\theta}{2\tau_p e^{-\gamma} + \frac{1}{2}(1 - e^{-\gamma})^2 + \Omega\sin\theta + \Gamma\cos\theta} \right] \tag{91}$$

using expression (89) for $H(\tau)$. The value of the final time at which flow takes place, τ_2^p, is determined by solving equations (77) and (89) to give

$$\tau_2^p = \tau_p + \sqrt{\frac{1-\tau_p}{2p_d^{2*}\beta}}\tan^{-1}\left(\frac{\Omega}{\Gamma}\right) \tag{92}$$

Thus, the final non-dimensional height of the hydrocarbon column is

$$H(\tau_2^p) = \frac{1}{1 - \frac{\rho_h}{\rho_w}} \times \left[p_c^* - p_d^{2*} + \sqrt{\frac{p_d^{2*}}{2\beta(1-\tau_p)}}\tan^{-1}\left(\frac{\Omega}{\Gamma}\right) \right] \tag{93}$$

In the limiting case $\beta \to \infty$, corresponding to the infinite period case $T \to \infty$, the final non-dimensional hydrocarbon column height, $H(\tau_2^p)$ approaches the limiting value given in equation (34) and hence it is not possible to exhaust the reservoir within a finite time. If $\beta \ll 1$, it can be shown that the non-dimensional critical depth, $s_c(\tau)$, decreases approximately linearly with non-dimensional time τ according to

$$s_c(\tau) \approx 1 - \frac{p_c^* - p_d^{2*}\left(\frac{1-\tau}{1-\tau_p}\right)}{1 - \frac{\rho_h}{\rho_w}} \tag{94}$$

over the interval $\tau_p \leq \tau \leq \tau_2^p$, from the maximum value given in equation (85) to zero at the time

$$\tau_2^p \approx 1 - \frac{1-\tau_p}{p_d^{2*}}\left(p_c^* - \left(1 - \frac{\rho_h}{\rho_w}\right)\right) \tag{95}$$

For the case of partial flow, the effective impulse imparted to the hydrocarbon, as defined earlier, is given by

$$I_p = \frac{1}{2}\left(1 - \frac{\rho_h}{\rho_w}\right)\int_{\tau_1^p}^{\tau_2^p} s_c(\tau)^2\, d\tau \qquad (96)$$

This impulse is directly proportional to the total decrease in hydrocarbon column height over the non-dimensional time interval $[\tau_1^p, \tau_2^p]$ according to the relationship (52), given explicitly as

$$I_p = \frac{1}{\beta}(1 - H(\tau_2^p)) \qquad (97)$$

If $\beta \ll 1$ then τ_2^p may be approximated by equation (95), the evolution of $s_c(\tau)$ over $\tau_1^p \le \tau \le \tau_p$ by the linear function (84) and the evolution of $s_c(\tau)$ over $\tau_p \le \tau \le \tau_2^p$ by the linear function (94). The time interval over which flow takes place is then

$$\tau_2^p - \tau_1^p \approx 1 - \frac{1}{p_d^{2*}}\left[p_c^* - \left(1 - \frac{\rho_h}{\rho_w}\right)\right] \qquad (98)$$

the effective impulse imparted to the fluid is

$$I_p \approx \frac{1}{6\left(1 - \frac{\rho_h}{\rho_w}\right)p_d^{2*}}\left[p_d^{2*} - p_c^* + \left(1 - \frac{\rho_h}{\rho_w}\right)\right]^3 \qquad (99)$$

and the decrease in hydrocarbon column height due to the linear pressure pulse function can be approximated using equation (97). This approximate measure of hydrocarbon migration can also be calculated by applying a $\beta \ll 1$ expansion to expression (93) for $H(\tau_2^p)$. It is clear that, for a constant value of β, the expression (99) for I_p and, hence, the amount of hydrocarbon migration, has its minimum value, namely 0, for a given value of p_c^* when $p_d^{2*} = p_c^* - \left(1 - \frac{\rho_h}{\rho_w}\right)$; this corresponds to the minimum peak of the pressure pulse function which will induce flow. Thus, as p_d^{2*} increases from $p_c^* - \left(1 - \frac{\rho_h}{\rho_w}\right)$ to p_c^*, a monotonic increase in hydrocarbon migration results. If p_d^{2*} takes the maximum value allowed by partial flow, the effective impulse is inversely proportional to $p_c^* = p_d^{2*}$:

$$I_p \approx \frac{1}{6p_c^*}\left(1 - \frac{\rho_h}{\rho_w}\right)^2 \qquad (100)$$

(iii) Complete flow over the fault plane:

At non-dimensional time $\tau = 0$ a non-dimensional pressure pulse function of the form (75) with peak value p_d^{3*} satisfying condition (69) (see Fig. 5) initiates a pressure increase within the hydrocarbon column. At the time τ_1^p, defined by

$$\tau_1^p = \frac{\tau_p}{p_d^{3*}}\left[p_c^* - \left(1 - \frac{\rho_h}{\rho_w}\right)\right] \qquad (101)$$

partial flow begins over the fault plane over a window $0 \le s \le s_c(\tau)$, where the critical depth is

$$s_c(\tau) = H(\tau) - \frac{p_c^* - p_d^{3*}\frac{\tau}{\tau_p}}{1 - \frac{\rho_h}{\rho_w}} \qquad (102)$$

and continues until the critical depth and non-dimensional hydrocarbon column height coincide at the non-dimensional time

$$\tau_1^c = \frac{p_c^*}{p_d^{3*}}\tau_p \qquad (103)$$

Flow takes place over the whole fault plane at non-dimensional times beyond τ_1^c as the pressure pulse function increases to a maximum at τ_p and subsequently decreases. This flow regime continues until the magnitude of the non-dimensional pressure pulse function falls to the value p_c^* at the non-dimensional time

$$\tau_2^c = 1 - \frac{p_c^*}{p_d^{3*}}(1 - \tau_p) \qquad (104)$$

Flow now ceases at the base of the hydrocarbon column and partial flow takes place over the fault plane at non-dimensional depths less than

$$s_c(\tau) = H(\tau) - \frac{p_c^* - p_d^{3*}\frac{1-\tau}{1-\tau_p}}{1 - \frac{\rho_h}{\rho_w}} \qquad (105)$$

until the migration of hydrocarbon across the fault plane stops at the non-dimensional time τ_2^p, defined implicitly by the relation

$$p_d^{3*}\frac{1 - \tau_2^p}{1 - \tau_p} = p_c^* - \left(1 - \frac{\rho_h}{\rho_w}\right)H(\tau_2^p) \qquad (106)$$

Following the approach presented and illustrated earlier, the four differential equations governing the evolution of $H(\tau)$ over the time intervals $\tau_1^p \le \tau \le \tau_1^c$, $\tau_1^c \le \tau \le \tau_p$, $\tau_p \le \tau \le \tau_2^c$ and $\tau_2^c \le \tau \le \tau_2^p$ can be solved analytically subject to the initial value $H(\tau_1^p) = 1$ and continuity of $H(\tau)$ at the non-dimensional times τ_1^c, τ_p and τ_2^c. It can be shown that the non-dimensional hydrocarbon column height has the following explicit solution for $\tau_1^p \le \tau \le \tau_p$:

$$H(\tau) = \frac{1}{1 - \frac{\rho_h}{\rho_w}}\left\{p_c^* - p_d^{3*}\frac{\tau}{\tau_p} + \sqrt{\frac{2p_d^{3*}}{\beta\tau_p}}\left(1 - 2\left[1 + e^{\sqrt{\frac{2\beta\tau_p}{p_d^{3*}}}\left(p_d^{3*}\frac{\tau}{\tau_p} - p_c^* + \left(1 - \frac{\rho_h}{\rho_w}\right)\right)}\right]^{-1}\right)\right\} \qquad (107)$$

for $\tau_1^p \leq \tau \leq \tau_1^c$,

$$H(\tau) = \frac{1}{1-\frac{\rho_h}{\rho_w}}\sqrt{\frac{\beta\tau_p}{2p_d^{3*}}}\, e^{-\frac{\beta p_d^{3*}}{2\tau_p}\left(\tau-\frac{p_c^*}{p_d^{3*}}\tau_p\right)^2} \times \left\{\left[1-2\left(1+e^{\sqrt{\frac{2\beta\tau_p}{p_d^{3*}}}\left(1-\frac{\rho_h}{\rho_w}\right)}\right)^{-1}\right]^{-1} + \frac{1}{2}\left(\frac{\tau_p}{p_d^{3*}}\right)^{\frac{1}{4}} \operatorname{erf}\left[\sqrt{\frac{\beta}{2}}\left(\frac{(p_d^{3*})^3}{\tau_p}\right)^{\frac{1}{4}}\left(\tau-\frac{p_c^*}{p_d^{3*}}\tau_p\right)\right]\right\}^{-1} \tag{108}$$

for $\tau_1^c \leq \tau \leq \tau_p$. For $\tau_p < \tau \leq \tau_2^p$, explicit expressions for $H(\tau)$ can also be derived as solutions of the systems: (i) the ordinary differential equation (36) over the non-dimensional time interval $\tau_p < \tau \leq \tau_2^c$ subject to the initial condition $H = H(\tau_p)$, defined using equation (108); and (ii) equation (32) over $\tau_2^c < \tau \leq \tau_2^p$ subject to the initial condition $H = H(\tau_2^c)$, defined using the solution (i) for H over the previous time interval. However, for this example, it is preferable to use a numerical procedure for the solution of these two systems which is applicable to any suitable pressure pulse function $F(\tau)$.

An explicit expression for the non-dimensional critical depth, $s_c(\tau)$, over the time interval $\tau_1^p \leq \tau \leq \tau_1^c$ follows from equations (102) and (107) and the approximate behaviour (84) for $\beta \ll 1$ is valid.

The value of the final time at which flow takes place, τ_2^p, and the final non-dimensional height of the hydrocarbon column $H(\tau_2^p)$ will be presented for particular examples of the non-dimensional parameters β, p_d^{3*} and p_c^*. An explanation of these results in terms of the total effective impulse imparted to the hydrocarbon so as to cause migration will also be given.

EXAMPLE: *a more complex pressure pulse function*

Over the time interval $0 \leq \tau \leq \tau_p$, the non-dimensional pressure pulse function increases from zero in direct proportion to t^α, where $\alpha > 0$, the peak value of pressure p_d^* then being achieved at $\tau = \tau_p$. An exponential decay in the pressure pulse function then follows until $\tau = 1$ when the pressure instantaneously returns to ambient, as shown in Fig. 6. The three different possible flow regimes can be described in a similar manner to the example of the linear pressure pulse function depicted in Fig. 5 with non-dimensional peak pressure values p_d^{2*} and p_d^{3*} corresponding to the partial flow and complete flow cases.

(i) Partial flow over the fault plane:
At non-dimensional time $\tau = 0$ the non-dimensional

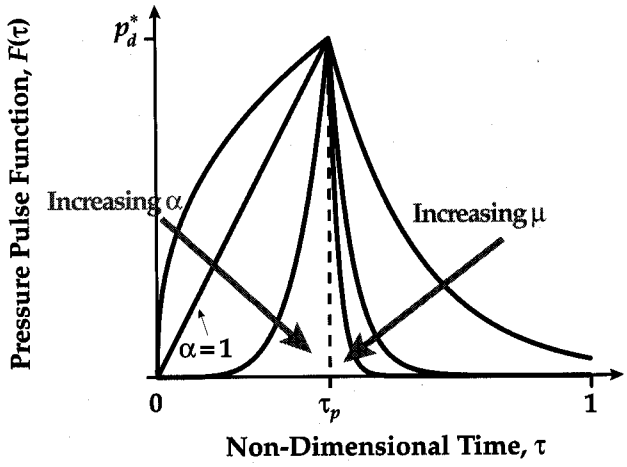

Fig. 6. *A more complex pressure pulse function which increases as τ^α, $\alpha > 0$, before decaying exponentially. The effect on the evolution of the function of varying the parameters α and ξ while keeping the peak pressure constant are indicated.*

pressure pulse function

$$F(\tau) = \begin{cases} p_d^{2*}\left(\dfrac{\tau}{\tau_p}\right)^\alpha, & \text{for } 0 \leq \tau \leq \tau_p \\ p_d^{2*} e^{-\xi(\tau-\tau_p)}, & \text{for } \tau_p \leq \tau \leq 1 \end{cases} \tag{109}$$

with peak value p_d^{2*} initiates a pressure increase within the hydrocarbon column. The value of the parameter ξ is assumed to be such that the pressure has almost returned to ambient at $\tau = 1$, the period of the pulse. Thus, if $F(1) < \frac{1}{1000}p_d^{2*}$, the parameter ξ would be constrained to be greater than $\frac{3\ln 10}{1-\tau_p}$.

The initial pressure increase causes flow over the fault plane at the time

$$\tau_1^p = \tau_p\left[\frac{p_c^* - \left(1-\frac{\rho_h}{\rho_w}\right)}{p_d^{2*}}\right]^{\frac{1}{\alpha}} \tag{110}$$

Condition (55) is satisfied and partial flow continues until the non-dimensional time τ_2^p, defined implicitly by the relation

$$p_d^{2*} e^{-\xi(\tau_2^p-\tau_p)} = p_c^* - \left(1-\frac{\rho_h}{\rho_w}\right)H(\tau_2^p) \tag{111}$$

assuming that the parameter ξ has been chosen to be sufficiently large. The largest depth at which flow occurs at any non-dimensional time $\tau_1^p \leq \tau \leq \tau_2^p$ is defined analogously to the linear pulse function in equation (78).

Following the approach given earlier, a solution of the differential equation (32) applied separately over the intervals $\tau_1^p \leq \tau \leq \tau_p$ and $\tau_p \leq \tau \leq \tau_2^p$ can be sought. However, it is preferable to use numerical techniques to derive the evolution of the non-dimensional hydrocarbon height and the results of this approach are presented later.

(ii) Complete flow over the fault plane:
At non-dimensional time $\tau = 0$ a non-dimensional pressure pulse function of the form (109) with peak value p_d^{3*} satisfying condition (69) initiates a pressure increase within the hydrocarbon column. At the time τ_1^p, defined similarly to expression (110), partial flow begins over the fault plane and continues until the critical depth and non-dimensional hydrocarbon column height coincide at the non-dimensional time

$$\tau_1^c = \left(\frac{p_c^*}{p_d^{3*}}\right)^{\frac{1}{\alpha}} \tau_p \qquad (112)$$

Flow takes place over the whole fault plane at non-dimensional times beyond τ_1^c as the pressure pulse function increases to a maximum at τ_p and subsequently decays exponentially. At the non-dimensional time

$$\tau_2^c = \tau_p + \frac{1}{\xi} \ln\left(\frac{p_d^{3*}}{p_c^*}\right) \qquad (113)$$

the magnitude of the non-dimensional pressure pulse function falls to the value p_c^* and partial flow is re-established. The migration of hydrocarbon across the fault plane stops at the non-dimensional time τ_2^p, defined implicitly by a relation similar to expression (111).

Rather than solving the four differential equations governing the evolution of $H(\tau)$ over the time interval $\tau_1^p \leq \tau \leq \tau_2^p$, we again utilise a numerical procedure and discuss the solution in terms of the non-dimensional parameters β, p_d^{3*} and p_c^* in the following section.

Numerical solutions and results

The analysis developed to model hydrocarbon migration across inactive faults was applied to three examples of possible pressure pulse functions. A full analytical investigation for the step and linear pressure pulse functions was made, whilst for the more complex function introduced the governing equations must be solved numerically. Thus, we first develop a numerical approach for solving the system of ordinary differential equations governing either partial flow, or complete flow, over the fault plane subject to a specified initial hydrocarbon column height.

NUMERICAL SOLUTIONS OF THE GOVERNING EQUATIONS

The ordinary differential equation and boundary conditions describing each system arising from the analysis of partial or complete flow over the fault plane, as described earlier, constitute simple two-point boundary-value problems. The NAG routine D02HBF is an algorithm for solving such two-point boundary-value problems in which the unknown parameters may be the boundary values and/or the range of integration. The estimated values of the parameters are corrected by a form of Newton iteration until convergence has been achieved to within a specified tolerance.

For the problems defined earlier, the unknown parameter will be either the final non-dimensional hydrocarbon column height at the end of the time interval or the time at which flow ceases, depending on which one of the following two situations is occurring:
(i) If the end of the time interval over which the integration is being carried out is known, i.e. the upper boundary is at τ_1^c, τ_p or τ_2^c, then the final non-dimensional hydrocarbon column height, i.e. $H(\tau_1^c)$, $H(\tau_p)$ or $H(\tau_2^c)$, will be the unknown parameter;
(ii) If the end of the time interval is unknown, i.e. the upper boundary is at τ_2^p, then the non-dimensional time at which flow ceases, τ_2^p, is the unknown parameter.

TYPICAL VALUES AND RANGES FOR FLOW PARAMETERS

The dimensional parameters governing the migration of hydrocarbon in the problems have specific values, or ranges of values, which determine the characteristics of the flow regime. Typical values of these governing dimensional parameters are listed prior to their interpretation in terms of ranges of values of the non-dimensional flow parameters β, p_d^* and p_c^*.

Dimensional flow parameters

The dimensional parameters governing the flow characteristics for hydrocarbon migration across a sealed fault plane have the following typical values:

Density of water, $\rho_w = 1035\ \text{kgm}^{-3}$;
Density of hydrocarbon, $\rho_h = 795\ \text{kgm}^{-3}$;
Acceleration due to gravity $g = 9.81\ \text{ms}^{-2}$;
Molecular viscosity, $\mu = 2\text{–}4$ cps $= 2 \times 10^{-3}$ – $4 \times 10^{-3}\ \text{Nsm}^{-2}$;
Horizontal surface area of reservoir, $A = 10^4\text{–}10^7\ \text{m}^2$;
Width of reservoir adjacent to fault, $l = 100\text{–}1000$ m;
Initial height of hydrocarbon column, $h_0 = 10\text{–}200$ m;
Thickness of sealed fault plane, $d = 1$ mm–10 cm;
Period of pressure pulse, $T = 1$ min–2 weeks $= 60\text{–}1.2096 \times 10^6$ s;
Permeability of fault rock, $K = 0.001\text{–}0.1$ mD;
Critical entry pressure, $p_c = 15\text{–}150$ psi $\approx 10^5\text{–}10^6\ \text{Nm}^{-2}$,

where 1 psi $= 6.89 \times 10^3\ \text{Nm}^{-2}$, 1 Darcy $= 9.869 \times 10^{-13}\ \text{m}^2$ and the range of thicknesses of the sealed fault plane reflects the fact that we are considering only an individual fault plane rather than a fault zone comprising a number of fault planes. The restriction (5) requires that the initial height of the hydrocarbon column h_0 satisfies the inequality:

$$h_0 \leq \frac{p_c}{(\rho_w - \rho_h)g} = 4.247 \times 10^{-4} p_c \qquad (114)$$

The upper bound (114) on the initial hydrocarbon column height corresponds to typical maximum initial hydrocarbon

columns of up to $h_{max} \approx 42$ ($p_c \approx 10^5$ Nm^{-2}) – 420 m ($p_c \approx 10^6$ Nm^{-2}) that can be supported by fault rocks whose permeabilities lie within the range $K = 0.001$ – 0.1 mD, respectively, as specified in the above parameter list.

Given an appropriate value for the critical entry pressure, condition (8) can be used to specify the minimum pulse amplitude, p_d, required to induce flow:

$$p_d > p_c - (\rho_w - \rho_h)gh_0 = p_c - 2354.4h_0 \qquad (115)$$

Thus, a critical entry pressure of $p_c = 10^6$ Nm^{-2} and an initial column height $h_0 = 200$ m, a pressure pulse with peak amplitude $p_d > 76.8$ psi $= 5.3 \times 10^5$ Nm^{-2} is required for the migration of hydrocarbon across the fault plane. If the peak of the pressure pulse function satisfies 5.3×10^5 Nm$^{-2} < p_d < 10^6$ Nm^{-2}, migration across the fault plane will take place but only over a portion of the hydrocarbon column, whilst, if $p_d \geq p_c = 10^6$ Nm^{-2} a period of complete flow will be achieved at some time within the duration of the pulse.

Non-dimensional flow parameters

The above values and ranges of dimensional parameters can be used to determine the following approximate range of values for the parameter β:

$$1.5 \times 10^{-12} \leq \beta \leq 0.3 \qquad (116)$$

The upper and lower bounds of the interval (116) correspond either to choosing values of the dimensional parameters K, h_0 and T at the upper and lower end of the ranges specified or, less significantly, choosing values of the dimensional parameters $\frac{A}{l}$, μ and d at the lower and upper end of their ranges, respectively. Increases in the value of the parameter β, whilst keeping p_c^* and p_d^* constant, correspond to increases in the level of the non-dimensional volume flowing across the fault plane.

Given values of the hydrocarbon and water densities, ρ_h and ρ_w, respectively, the constraint (29), corresponding to the upper limit (5) on the initial hydrocarbon column height when in dimensional variables, requires that $p_c^* \geq 0.2319$.

From typical values of the dimensional critical pressure p_c and the corresponding appropriate initial hydrocarbon column heights h_0 satisfying the constraint (114), the following range of values of the non-dimensional critical pressure has been determined:

$$0.2319 \leq p_c^* \leq 10 \qquad (117)$$

where the upper bound arises from a typical minimum hydrocarbon column height of 10 m. It should be noted that the value of p_c^* varies only according to the ratio $\frac{p_c}{h_0}$ so that for any hydrocarbon reservoir which is at its limiting maximum initial column height, always, $p_c^* = 0.2319$. Furthermore, as p_c^* is inversely proportional to h_0, it measures the relative initial capacity of the reservoir in comparison to the maximum capacity for a given fault rock critical entry pressure. Thus, larger values of p_c^* correspond to reservoirs under which the fault rock is subjected to relatively smaller ambient pressure differences, i.e. h_0 is much less than the maximum that could be held back by the fault rock and, hence, these reservoirs are less susceptible to hydrocarbon migration under the influence of a pressure pulse with a given amplitude.

The conditions (54), (55) and (69), which define the ranges of values of the parameter p_d^* corresponding to the non-dimensional peak of the pressure pulse function for the situations in which no flow, partial flow and complete flow, respectively, exist over the fault plane, can be summarised as follows:

$$\begin{aligned}
&\text{No flow: } 0 < p_d^* \leq p_c^* - \left(1 - \frac{\rho_h}{\rho_w}\right) = p_c^* - 0.2319 \\
&\text{Partial flow: } p_c^* - \left(1 - \frac{\rho_h}{\rho_w}\right) < p_d^* < p_c^* \\
&\qquad \text{or } p_c^* - 0.2319 < p_d^* < p_c^* \\
&\text{Complete flow: } p_d^* \geq p_c^* \qquad (118)
\end{aligned}$$

FLOW MODEL RESULTS

This section will compare the predicted loss of non-dimensional hydrocarbon column height $(1 - H(\tau))$ achieved for a range of values of the parameters β, p_c^* and p_d^* within the three models for the pressure pulse function examined earlier. An additional set of parameters governing the evolution of the pressure pulse function will also be discussed. Thus, both the evolution and the final loss of non-dimensional hydrocarbon column height will be investigated as the parameter τ_p for the linear function and the parameters τ_p, α and ξ for the complex function are varied. To explain the variation in the migration of hydrocarbon through the fault plane, some results from the present section will be translated back into dimensional quantities.

The predicted evolutions of the non-dimensional hydrocarbon column height presented here will be based upon the following sets of parameter values lying within the ranges (116) and (117) and satisfying conditions (118):

$$\beta_1 = 0.3, \quad \beta_2 = 2 \times 10^{-6}, \qquad (119)$$

non-dimensional critical entry pressures:

$$p_c^{*1} = 0.25, \quad p_c^{*2} = 4, \quad p_c^{*3} = 9, \qquad (120)$$

and non-dimensional peak pressures:

$$\begin{aligned}
&p_d^{*11} = 0.15, \quad p_d^{*21} = 3.85, \quad p_d^{*31} = 8.85, \\
&p_d^{*12} = 2.0, \quad p_d^{*22} = 6.0, \quad p_d^{*32} = 12.0 \qquad (121)
\end{aligned}$$

where the notation p_d^{*ij} denotes the peak pressure giving partial flow for $j = 1$ and complete flow for $j = 2$ when the critical entry pressure is p_c^{*i}.

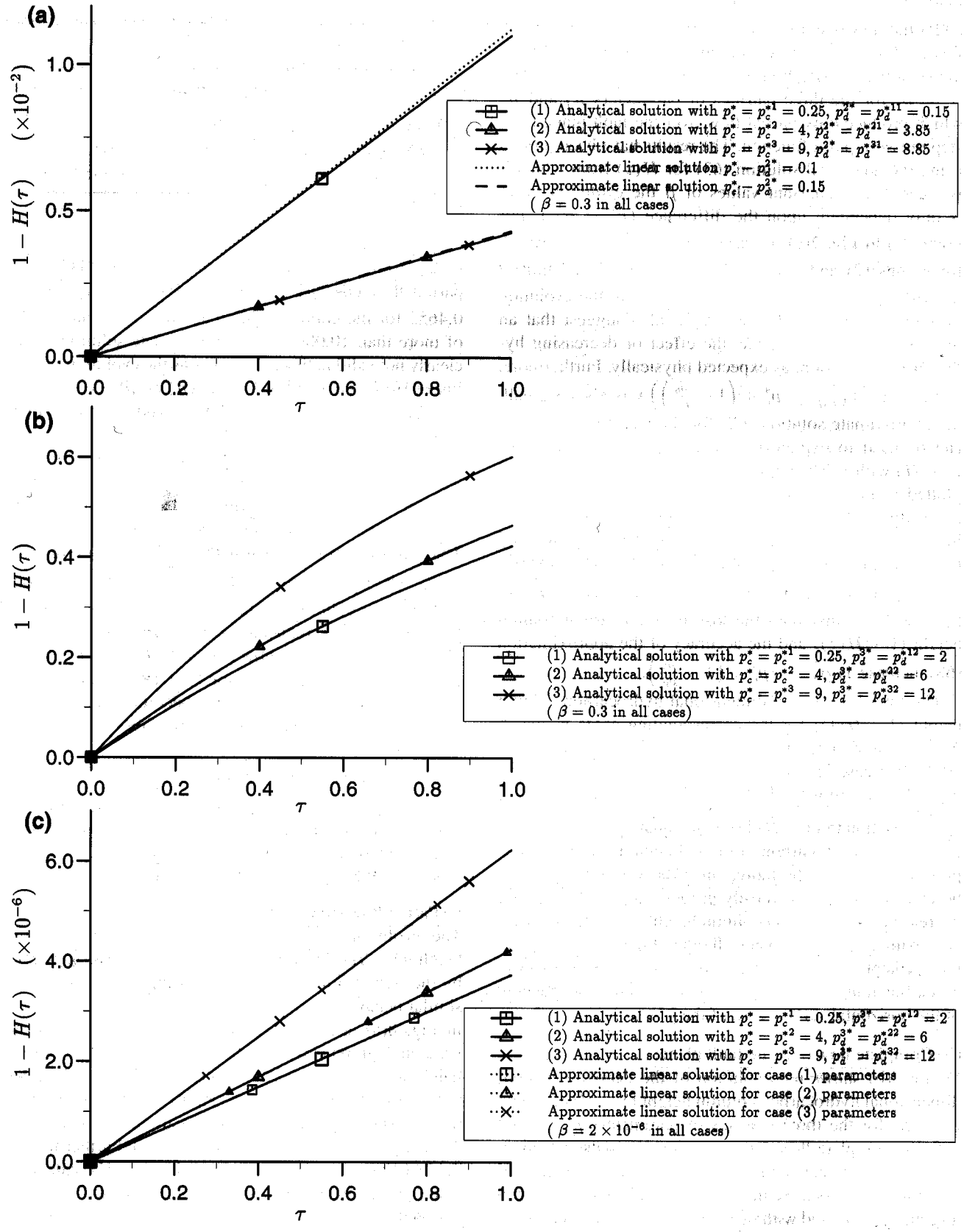

Fig. 7. *The evolution of the decrease in non-dimensional hydrocarbon column height, $(1 - H(\tau))$, with non-dimensional time, τ, for the step pressure pulse function at a variety of sets of flow parameters.*

Example: the step pressure pulse function

(i) Partial flow over the fault plane:

Figure 7(a) shows the evolution of the decrease in non-dimensional hydrocarbon column height, $(1-H(\tau))$, when $\beta = \beta_1$ for the three pairings of parameters p_d^* and p_c^* which produce only partial flow over the fault plane for a step pressure pulse function. The results have been plotted using the analytical solution (63) for $H(\tau)$ from which it is clear that at constant values of β the evolution of H is only dependent upon the difference $(p_c^* - p_d^{2*})$. For graph (1) in Fig. 7(a) we have $(p_c^* - p_d^{2*}) = 0.1$ whilst for graphs (2) and (3) $(p_c^* - p_d^{2*}) = 0.15$ and thus if the difference $(p_c^* - p_d^{2*})$ remains constant the evolution of $H(\tau)$ is unchanged. The graphs also suggest that an increase in $(p_c^* - p_d^{2*})$ has the effect of decreasing hydrocarbon migration, as expected physically. Furthermore, as the term $\beta\left(p_d^{2*} - p_c^* + \left(1 - \frac{\rho_h}{\rho_w}\right)\right)\tau$ is always small, the approximate solution (68) for the step function pulse can be used to explain the linearity of the evolution of $(1-H)$ with τ. The approximate solutions (68) have been plotted in Fig. 7(a) to confirm the close agreement with the analytical solution (63) which improves as $(p_c^* - p_d^{2*})$ increases. It is also clear from equation (68) that, provided this approximation is valid, the value of $(1-H(\tau))$ varies as the square of the difference $\left(\left(1 - \frac{\rho_h}{\rho_w}\right) - (p_c^* - p_d^{2*})\right)$ thus verifying that both the loss in hydrocarbon column height $(1-H(\tau))$ and the accuracy of the approximation (68) increase as $p_d^{2*} \to p_c^* - \left(1 - \frac{\rho_h}{\rho_w}\right)$.

The total loss in non-dimensional hydrocarbon column height $(1-H(1))$ for the corresponding cases in which $\beta = \beta_2$ is reduced by a factor of approximately 6.8×10^{-6}. For cases in which $\beta \ll 1$, and hence the term $\beta\left(p_d^{2*} - p_c^* + \left(1 - \frac{\rho_h}{\rho_w}\right)\right)$ is small, we can deduce an approximation to $(1-H(1))$ from equation (68), whereby the loss in hydrocarbon column height is directly proportional to β. Furthermore, since the variation in β can be considered to be inversely proportional to A, the total decrease in hydrocarbon column height $(1-H(1))$ varies approximately as A^{-1}, when all other dimensional parameters are kept constant. Thus, the dimensional volume of hydrocarbon migration $Ah_0(1-H(1))$ becomes independent of the horizontal surface area of the reservoir if $\beta \ll 1$.

(ii) Complete flow over the fault plane:

Figure 7(b) shows the evolution of the decrease in non-dimensional hydrocarbon column height $(1-H(\tau))$ when $\beta = \beta_1$ for the three pairings of parameters p_d^* and p_c^* defining complete flow for a step pressure pulse function. The results presented in this figure using the analytical solution (72) emphasise the large increases in hydrocarbon migration compared with the situation of partial flow as we increase the size of the step pressure pulse function beyond p_c^* to a value for which flow is achieved at all depths. For instance, with $p_c^* = 4$, the loss in non-dimensional hydrocarbon column height $(1-H(1))$ is 0.0043 for the partial flow case $p_d^{2*} = 3.85$ whilst this height loss is 0.4652 for the complete flow case $p_d^{2*} = 6$, an increase of more than 10,000%. The approximate solution (73) is clearly not valid in these examples as the evolutions are not linear. However, as the difference $(p_d^{3*} - p_c^*)$ decreases the linearity of the graphs does improve and the migration of hydrocarbon is reduced.

Table 1. A comparison of the predicted, analytical solution for the decrease in hydrocarbon column height $(1-H(1))$ with the $\beta \ll 1$ approximation valid for partial flow when $\beta = 0.3$.

p_d^{2*}	p_c^*	$\beta \ll 1$ approximation	$1 - H(\tau_2^p)$
0.15	0.25	3.298×10^{-3}	3.269×10^{-3}
3.85	4.0	3.077×10^{-5}	3.075×10^{-5}
8.85	9.0	1.338×10^{-5}	1.338×10^{-5}

The same set of parameters as used in Fig. 7(b) were used in Fig. 7(c) for the case $\beta = \beta_2$. The approximate solution (73) has been superimposed on the graphs in each case and these two plots are graphically indistinguishable. Thus, the evolution is linear with τ and in direct proportion to $p_d^{3*} - p_c^* + \frac{1}{2}\left(1 - \frac{\rho_h}{\rho_w}\right)$. The total loss in non-dimensional hydrocarbon column height $(1-H(1))$ as β is reduced from β_1 to β_2 is reduced by a factor of approximately 10^{-5}. As for the partial flow case, if $\beta \ll 1$, approximately $(1-H(1)) \propto \beta$, from equation (73), and the dimensional volume of hydrocarbon migration becomes independent of the horizontal surface area of the reservoir.

Example: the linear pressure pulse function

In the majority of cases discussed for this example, and unless otherwise stated, the peak of the linear pressure pulse function is assumed to occur at the non-dimensional time $\tau_p = 0.5$.

(i) Partial flow over the fault plane:

The evolution of the decrease in hydrocarbon column height $(1-H(\tau))$ for the sets of parameter values defined by the partial flow cases (1)–(3) in Fig. 7(a) show a very similar behaviour to the complete flow examples presented in Fig. 8(a) and discussed below. These results are not presented graphically, as the final hydrocarbon column height losses for cases (2) and (3) are a factor of less than 0.01 of the height loss in case (1); instead the total increase in $(1-H)$ due to these linear pressure pulse functions in Table 1, when $\beta = 0.3$, are demonstrated. Furthermore, in Table 1 the approximate increases in $(1-H)$, calculated using expressions (97) and (99), are presented under the assumption that $\beta \ll 1$, which is a valid assumption for the ranges of non-dimensional parameters used here. The agreement between the $\beta \ll 1$ solution and the analytical solution (93) is good for the cases presented.

The results for $\beta = \beta_2$ show very similar behaviour to the β_1 case and migration of hydrocarbon is reduced by a factor of approximately 6.7×10^{-6} compared to the corresponding $\beta = \beta_1$ cases. This reduction factor is of approximately the same magnitude as that observed for partial flow due to a step pressure pulse function. A comparison of the total decrease in hydrocarbon column height $(1 - H(1))$ with the $\beta \ll 1$ approximations, as presented for $\beta = \beta_1$ in Table 1, again confirms their excellent agreement.

(ii) Complete flow over the fault plane:
The evolution of the loss in non-dimensional hydrocarbon column height $(1 - H(\tau))$ for the three sets of parameter values defined in Fig. 7(b) has been used in Fig. 8(a) to demonstrate its behaviour under the influence of a variety of linear pressure pulse functions which develop complete flow over the fault plane. The times τ_2^p at which flow ceases are indicated for each of the graphs. The analytical solutions (107) and (108) which define the function $(1 - H(\tau))$ over the time interval $\tau_1^p \leq \tau \leq \tau_p$ have been calculated in each case and excellent agreement between the numerical and analytical solutions was found. As the difference cannot be discerned graphically, only the analytical results are shown in Fig. 8(a).

The total loss in non-dimensional hydrocarbon column height $(1 - H(1))$ as β is reduced from β_1, shown in Fig. 8(a), to β_2 is reduced by a factor of approximately 10^{-5}, the same factor observed for the step pressure pulse function.

As expected, the profile of $(1 - H(\tau))$ as time evolves is quite different to the profiles shown in Fig. 7 for the step pressure pulse function and the overall migration of hydrocarbon is reduced in all cases. However, the important difference between Figs. 7(b) and 8(a) is that for the step pressure pulse there is a monotonic decrease in hydrocarbon migration as the difference $(p_d^{3*} - p_c^*)$ is reduced, whilst for the linear pressure pulse the relationship between $(p_d^{3*} - p_c^*)$ and the amount of hydrocarbon which migrates must be more complex. For the cases in which partial flow only is achieved due to the linear pressure pulse, some analysis was carried out and it was shown that the increase in $(1 - H(\tau))$ is proportional to both the cube of $\left(p_d^{2*} - p_c^* + \left(1 - \frac{\rho_h}{\rho_w}\right)\right)$ and inversely proportional to p_d^{2*} itself, assuming that the $\beta \ll 1$ approximation is valid. Clearly, a similar type of relationship must exist for the case of complete flow but, without an explicit expression for the evolution of $H(\tau)$, it is possible only to demonstrate the variation with τ of

$$\int p_{eff}\, ds \tag{122}$$

the area under this curve representing the evolution of the effective impulse $I_p(\tau)$ which is proportional to the decrease in hydrocarbon column height $(1 - H(\tau))$. The limits of the integral depend on whether complete flow or partial flow is occurring at that time. Thus, Fig. 8(b) presents the evolution of the function (122) with non-dimensional time τ for the three variations in the parameters p_d^{3*} and p_c^* used in Fig. 8(a) when $\beta = 0.3$. The area under the curve for case (1) is clearly the greatest, showing that, despite $(p_d^{3*} - p_c^*)$ being smaller than for the other two cases, this set of parameter values gives the greatest hydrocarbon migration in comparison to cases (2) and (3).

It is evident from Figs. 7(b) and 8(a) and a comparison of the results in Fig. 7(a) with those in Table 1 that the migration of hydrocarbon across the fault plane under the same set of non-dimensional parameters depends crucially on the model we choose for the profile of the pressure pulse function. Not only does the evolution of the function $(1 - H(\tau))$ change significantly and the amount of hydrocarbon migration reduce when we transfer from the step function to the linear function model, but also the dependence upon the non-dimensional critical entry pressure and peak of the pressure pulse function is quite different.

The variation of $H(\tau)$ with τ_p.
In Fig. 9 the non-dimensional parameters β, p_c^* and p_d^* have been kept at the constant values $\beta = \beta_1 = 0.3$, $p_c^* = p_c^{*1} = 0.25$ and $p_d^{2*} = p_d^{*11} = 0.15$ so that partial flow takes place over the time interval $[\tau_1^p, \tau_2^p]$ but the time at which the linear pressure pulse function reaches its peak value is varied within the range $\tau_p \in (0, 1)$. We have taken $\tau_p = 0.1$, 0.3, 0.5, 0.7 and 0.9 and plotted the associated profiles of $(1 - H(\tau))$ with τ. The time intervals over which flow takes place, $(\tau_2^p - \tau_1^p)$, and the loss in hydrocarbon column height $(1 - H(\tau_2^p))$ over this interval are graphically indistinguishable, although they are not identical. If this value of β is sufficiently small for the $\beta \ll 1$ approximations derived earlier to apply, then equations (98) and (99) demonstrate that in such situations both the time interval for flow and the overall loss of hydrocarbon column height $(1 - H(1))$, respectively, will both be independent of the value of the parameter τ_p.

Precisely the same observations were recorded for the case of complete flow for which the peak of the linear pressure pulse function was increased to $p_d^{3*} = p_d^{*12} = 2$. However, the result in this case could not be demonstrated analytically as a numerical approach was employed in the solution of the governing equations.

Example: the more complex pressure pulse function

Unless otherwise stated, in the cases discussed for this example the peak of the complex pressure pulse function occurs at the non-dimensional time $\tau_p = 0.5$ and the parameters $\alpha = 0.4$ and $\xi = 10$. Beyond $\tau = \tau_p$ the pressure pulse function decays exponentially according to the parameter ξ and the value $\xi = 10$ was necessary to ensure that flow ceased before $\tau = 1$ for all combinations of the non-dimensional flow parameter values given in equations (119)–(121).

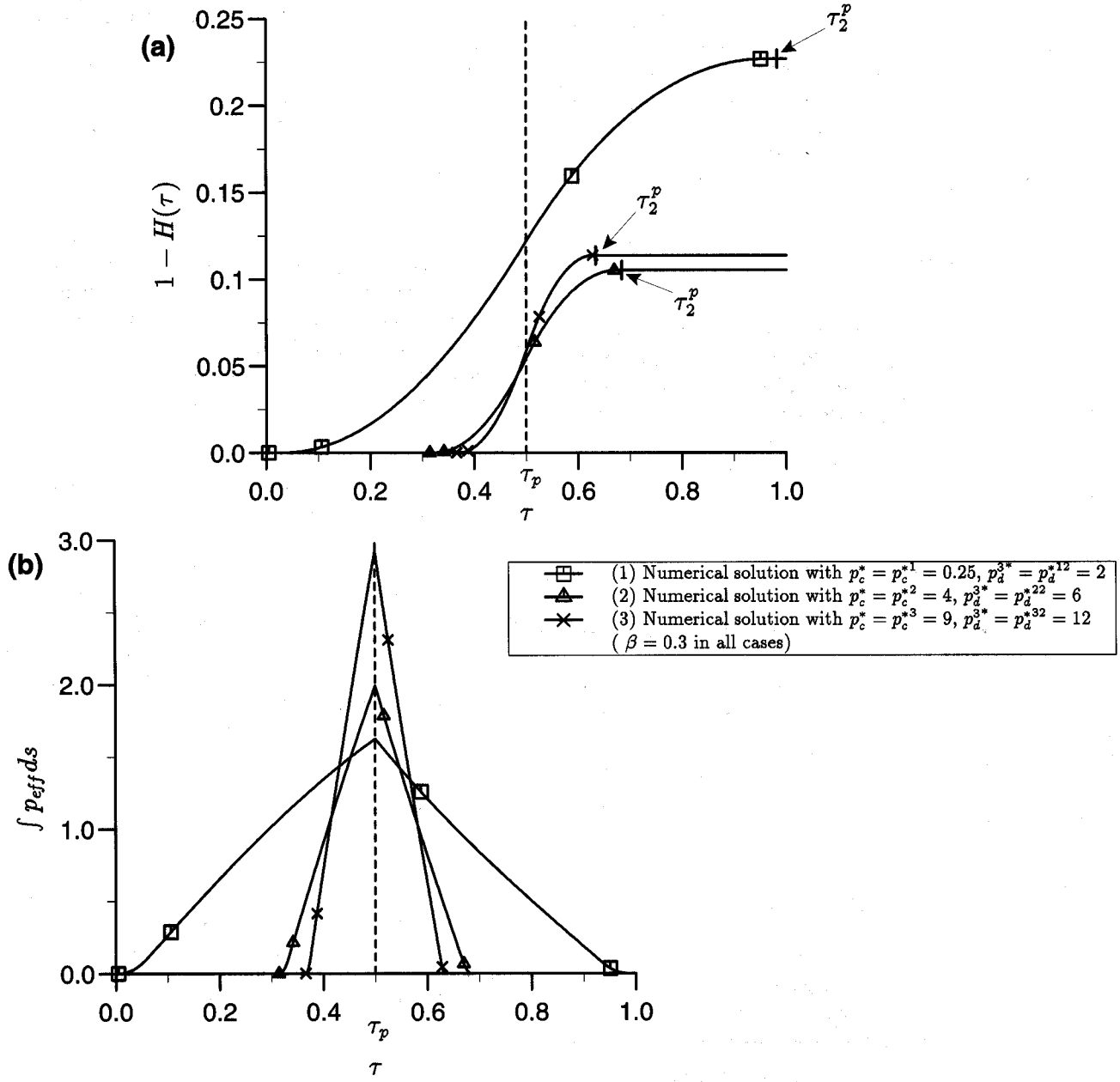

Fig. 8. *Particular sets of parameters defining complete flow over the fault plane for the linear pressure pulse function: (a) the evolution of* $(1 - H(\tau))$*; and, (b) the evolution of the function* $\int p_{eff} ds$ *with* τ.

The behaviour of the loss in non-dimensional hydrocarbon column height $(1 - H(\tau))$ as we vary the parameters β, p_c^* and p_d^* according to the values in equations (119)–(121) is very similar to the results obtained for the linear pressure pulse function, in the cases of both partial and complete flow. To illustrate this point, and also some typical profiles of the evolution of $(1 - H(\tau))$ with τ, Fig. 10 gives the results obtained for the complex pressure pulse function in the cases of complete flow shown for the linear pressure pulse function in Fig. 8(a).

The variation of $H(\tau)$ with τ_p, α and ξ.

The brief discussion that follows determines the impact of independent variations in each of the non-dimensional parameters τ_p, α or ξ governing the profile of the complex pressure pulse function on the migration of hydrocarbon across the fault plane.

In Fig. 11(a) the non-dimensional flow parameters β, p_c^* and p_d^* have been kept at the constant values $\beta = \beta_1 = 0.3$, $p_c^* = p_c^{*2} = 4$ and $p_d^{3*} = p_d^{*22} = 6$ so that complete flow takes place, and the parameter values $\alpha = 0.4$ and $\xi = 10$ are used to define the profile of $F(\tau)$. The time at which the complex pressure pulse function reaches its peak value is now varied within the range $\tau_p \in (0, 1)$ to produce different profiles of $(1 - H(\tau))$ with τ. As

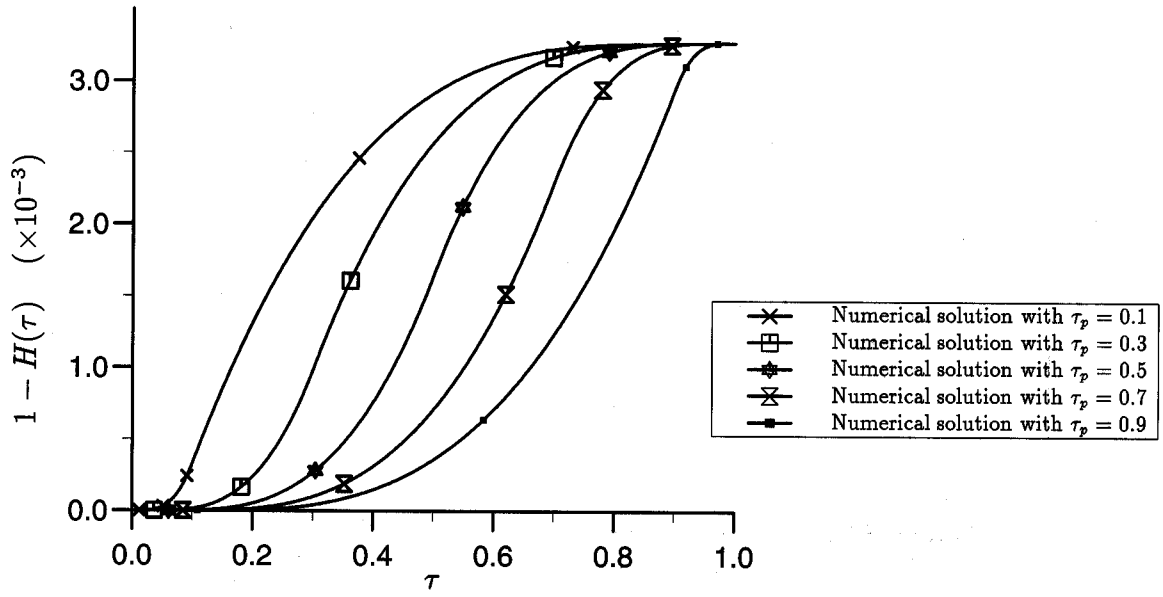

Fig. 9. *The variation in hydrocarbon migration* $(1 - H(\tau))$ *and flow period with the time,* τ_p*, at which the linear pressure pulse function achieves its peak value for the non-dimensional parameters* $\beta = 0.3$, $p_c^* = p_c^{*1} = 0.25$ *and* $p_d^{2*} = p_d^{*11} = 0.15$.

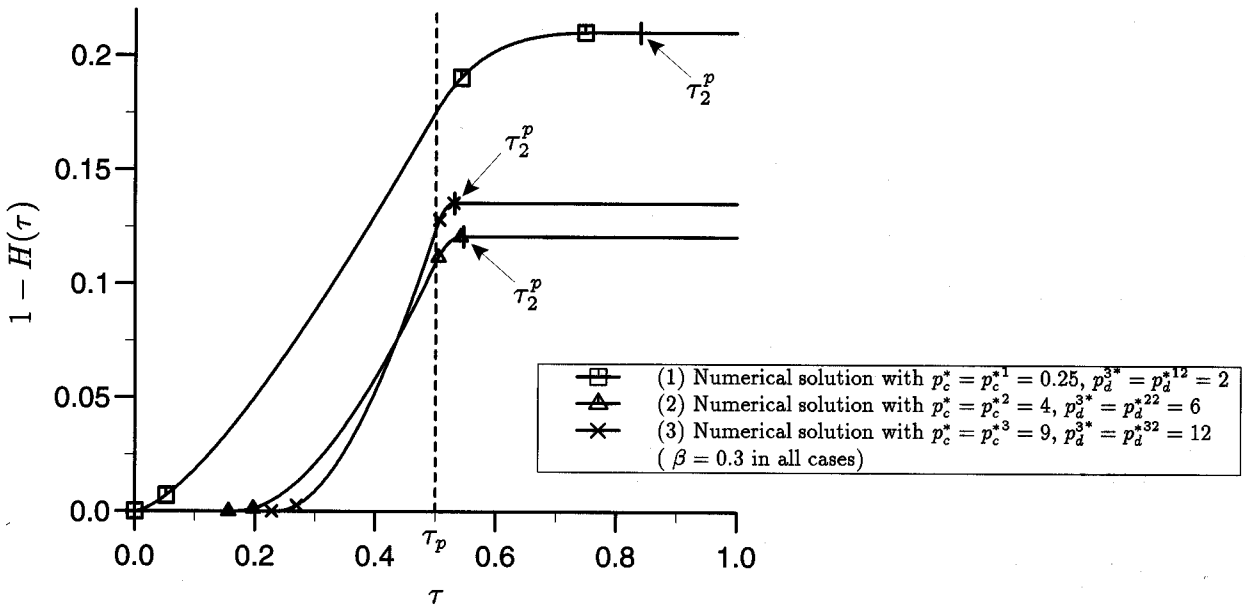

Fig. 10. *The evolution of the decrease in non-dimensional hydrocarbon column height* $(1 - H(\tau))$ *with* τ *for a complete flow situation and the complex pressure pulse function.*

predicted by equation (110), the value of τ_1^p increases linearly with τ_p. The values of the time at which flow ceases, τ_2^p, and the loss in hydrocarbon column height over the interval $[\tau_1^p, \tau_2^p]$, namely $(1 - H(\tau_2^p))$, also increase approximately linearly as we increase τ_p. In all cases, the flow beyond $\tau = \tau_p$ is identical and, thus, there is an approximately linear dependence of $(1 - H(\tau_p))$ on τ_p which would become clear from an analytical investigation of the governing differential systems at small values of β. The fact that an increase in τ_p results in greater hydrocarbon migration follows from a consequential increase in the area under $F(\tau)$ and hence an increase in the effective impulse imparted to the hydrocarbon. Clearly, the characteristics of the same investigation applied to the partial flow case are very similar.

Using the same flow parameters as for Fig. 11(a) and with $\tau_p = 0.5$ and $\xi = 10$, the variation of hydrocarbon migration with the parameter α is determined for complete flow in Fig. 11(b). The most interesting observations for this example are: (i) $\alpha \to \infty$ approaches the case of

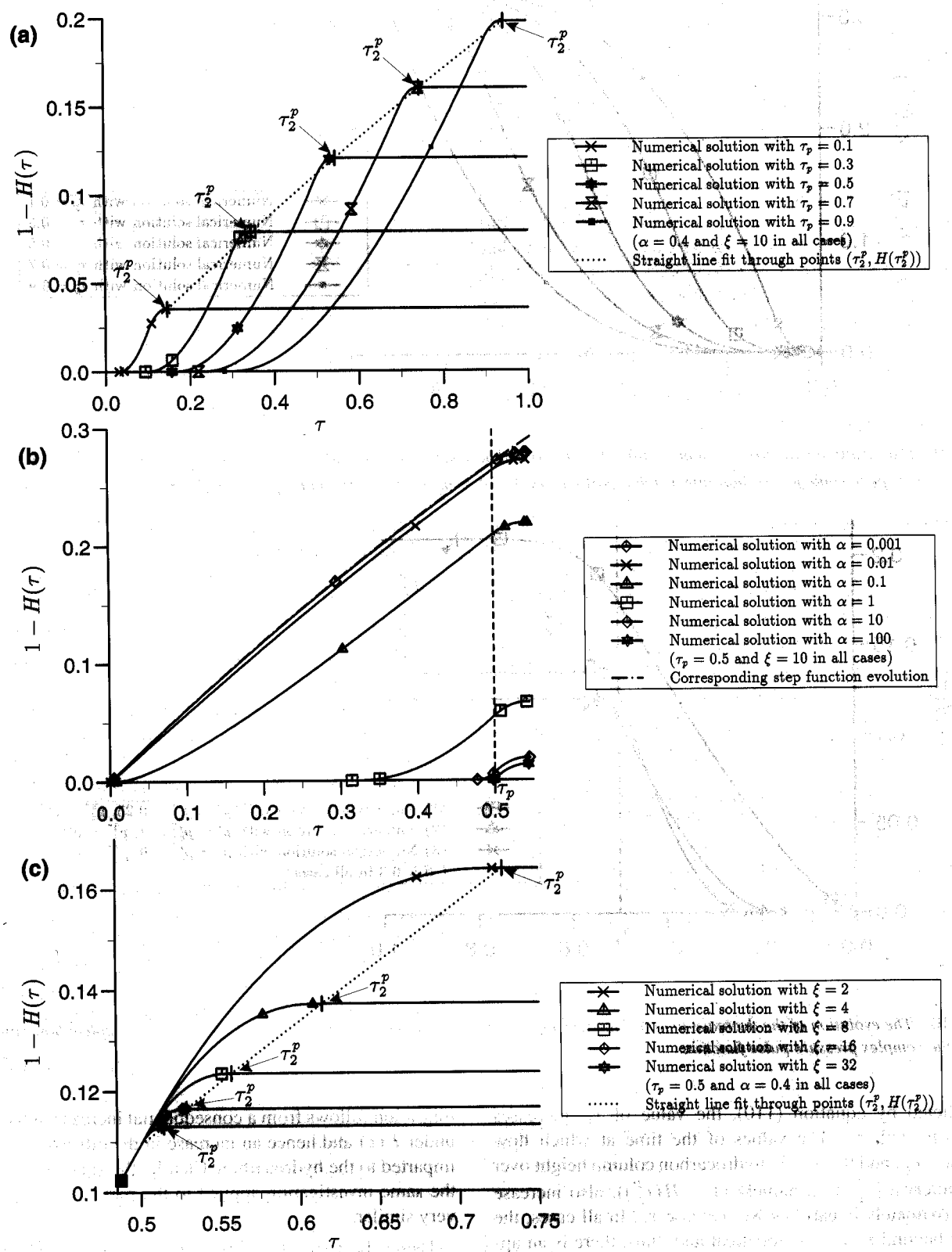

Fig. 11. *The impact on the migration of hydrocarbon across the fault plane of variations in each of the parameters τ_p, α and ξ defining the profile of the complex pressure pulse function for $\beta = 0.3$, $p_c^* = p_c^{*2} = 4$ and $p_d^{3*} = p_d^{*22} = 6$.*

no flow over the time interval $[0, \tau_p]$; (ii) for $\alpha \to 0$ the pressure pulse function, $F(\tau)$, and the profile of $(1 - H(\tau))$ both approach their corresponding cases for the step function over $[0, \tau_p]$; and, (iii) $\alpha = 1$ gives results for the corresponding linear pressure pulse function over $[0, \tau_p]$. A reduction in p_d^* to the partial flow case shows that the same rate of decrease of α results in a more rapid relative decrease in hydrocarbon migration $(1 - H(1))$, as predicted by equation (110).

Figure 11(c) presents the variation of the decrease in hydrocarbon column height $(1 - H(\tau))$ beyond the time $\tau_p = 0.5$, using $\alpha = 0.4$, as the parameter ξ is varied when the same flow parameters as used in Figs. 11(a) and 11(b) are employed. Thus, complete flow is occurring although the results for partial flow show the same characteristics. The expected reduction in hydrocarbon migration as ξ is increased is such that the values of τ_2^p and $(1 - H(\tau_2^p))$ decrease whilst the functions $(\tau_2^p - \tau_p)$ and $[(1 - H(\tau_2^p)) - (1 - H(\tau_p))]$ remain approximately linearly related.

ESTIMATED HYDROCARBON PRODUCTION RATES

A complete specification of a hydrocarbon reservoir and the bounding inactive fault in terms of the viscosity of the hydrocarbon, μ, the thickness of the fault rock, d, the ratio of the horizontal surface area of the reservoir to the horizontal length of the fault over which there is the potential for leakage, $\frac{A}{l}$, the permeability of the fault rock, K, and the critical entry pressure of the fault rock, p_c, provides the platform for a discussion of the application of the model presented in this paper. The remaining dimensional parameters which affect the volume of hydrocarbon migration are (i) the initial hydrocarbon column height, h_0, which is constrained to be less than h_{max}, defined in equation (114), according to properties of the fault rock; (ii) the peak value achieved by the applied pressure pulse function, p_d, which governs whether flow exists and, if it does, over what depth migration takes place; and, (iii) the model profile for the pressure pulse function, three examples of which have been demonstrated earlier.

A hydrocarbon reservoir with $\beta = 0.3$

Suppose the hydrocarbon reservoir and fault rock to have the following dimensional properties:

$$\mu = 2 \times 10^{-3}\ \text{Nsm}^{-2}, \quad d = 10^{-3}\ \text{m}, \quad \frac{A}{l} = 100\ \text{m}$$
$$T = 1.2 \times 10^6\ \text{s}, \quad K = 0.1\ \text{mD} = 9.869 \times 10^{-17}\ \text{m}^2 \tag{123}$$

in accordance with the dimensional parameter ranges defined earlier. By taking the critical entry pressure as

$$p_c = 1.2666 \times 10^5\ \text{Nm}^{-2} \tag{124}$$

the maximum hydrocarbon column height which can be supported by the fault rock is

$$h_{max} = 53.793\ \text{m} \tag{125}$$

from expression (114). To ensure that the non-dimensional parameter β, defined in equation (27), takes the value $\beta = 0.3$ the initial hydrocarbon column height is chosen to be

$$h_0 = 49.8985\ \text{m} \tag{126}$$

As a direct result of the choice (124) for the critical entry pressure, approximately, $p_c^* = 0.25$. Thus, the flow regimes specified in equation (118) require that

$$p_d^* \le 0.0181 \quad \text{or} \quad p_d \le 9170.1\ \text{Nm}^{-2} \quad \text{or} \quad p_d \le 1.33\ \text{psi} \tag{127}$$

for no flow,

$$0.0181 < p_d^* < 0.25 \quad \text{or} \quad 9170.1 < p_d < 1.2666 \times 10^5\ \text{Nm}^{-2} \quad \text{or} \quad 1.33 < p_d < 18.38\ \text{psi} \tag{128}$$

for partial flow only and

$$p_d^* \ge 0.25 \quad \text{or} \quad p_d \ge 1.2666 \times 10^5\ \text{Nm}^{-2} \quad \text{or} \quad p_d \ge 18.38\ \text{psi} \tag{129}$$

to achieve complete flow. Table 2 shows the volume of hydrocarbon migration

$$\tilde{V} = A(h_0 - h(T)) = Ah_0(1 - H(1)) \tag{130}$$

as defined in equation (21), which may be achieved under the above set of parameters. Given that $\frac{A}{l} = 100$ m in the parameter definitions (123) and $A = 10^4\ \text{m}^2$, the total hydrocarbon migration volume for the examples $p_d^* = 0.15$ and $p_d^* = 2$ has been presented. The results from all three models for the pressure pulse function have been included and the parameters governing their profile are precisely the ones given earlier.

A hydrocarbon reservoir with $\beta = 2 \times 10^{-6}$

The results given in Table 2 demonstrate the process described in this paper in which the model parameters, and hence the predicted hydrocarbon migration, are at the upper extreme of their likely values. In the next example, the process is illustrated using a set of dimensional parameters in which the migration of hydrocarbon is much less, namely

$$\mu = 3 \times 10^{-3}\ \text{Nsm}^{-2}, \quad d = 10^{-2}\ \text{m}, \quad \frac{A}{l} = 1000\ \text{m}$$
$$p_c = 4.1413 \times 10^5\ \text{Nm}^{-2},$$
$$K = 6 \times 10^{-18}\ \text{m}^2 = 0.00608\ \text{mD} \tag{131}$$
$$h_0 = 10.197\ \text{m} < h_{max} = 175.881\ \text{m},$$
$$T = 96586.90\ \text{s} = 1.118\ \text{days}$$

so that $\beta = 2 \times 10^{-6}$ and $p_c^* = 4.0$. Taking $A = 5 \times 10^5\ \text{m}^2$ Table 3 presents the total hydrocarbon migration volume for the examples $p_d^* = 3.85$ and $p_d^* = 6$ using the results for all three models for the pressure pulse function given earlier.

Table 2. Hydrocarbon migration volumes for models of the pressure pulse with period approximately 2 weeks and peaks corresponding to partial and complete flow.

Pulse model	p_d^*	p_d ($\times 10^5$ Nm^{-2})	Flow regime	$1 - H(1)$	Volume (m^3)	Volume (bbls)
Step				1.1033×10^{-2}	5505.35	34,650
Linear	0.15	0.7600	Partial	3.2691×10^{-3}	1631.24	10,260
Complex				3.3210×10^{-3}	1657.12	10,420
Step				0.42403	211584.61	1,330,870
Linear	2.0	10.1327	Complete	0.22710	113319.49	712,780
Complex				0.21057	105071.27	660,900

Table 3. Hydrocarbon migration volumes for models of the pressure pulse with period approximately 1.1 days and peaks corresponding to partial and complete flow.

Pulse model	p_d^*	p_d ($\times 10^5$ Nm^{-2})	Flow regime	$1 - H(1)$	Volume (m^3)	Volume (bbls)
Step				2.8915×10^{-8}	0.147	0.92
Linear	3.85	3.9860	Partial	2.0500×10^{-10}	1.045×10^{-3}	6.57×10^{-3}
Complex				2.7482×10^{-10}	1.401×10^{-3}	8.81×10^{-3}
Step				4.2319×10^{-6}	21.576	135.7
Linear	6.0	6.2120	Complete	7.4695×10^{-7}	3.808	24.0
Complex				8.6177×10^{-7}	4.394	27.6

Conclusions

The new model has been analysed in detail for the process by which inactive faults can allow hydrocarbons to migrate across them when activity on an adjacent fault induces a pressure pulse; high production rates have been demonstrated over the time period for which the fluid pressure difference is above the critical entry pressure. After presenting a full description of this system, the behaviour of the hydrocarbon reservoir under the influence of the pressure pulse was determined either analytically or numerically for three separate models of the profile of the pulse. Results have been obtained over a range of non-dimensional parameters which demonstrate both high and low amounts of migration when interpreted in the original dimensional variables.

Given the typical dimensional reservoir parameters, the predicted volume of hydrocarbon migration due to any of the three models of the pressure pulse can now be predicted readily. In reality, such pressure pulses often occur not just as single entities, but rather as a train of pulses over short intervals. However, from the parameters specifying the reservoir, the bounding fault rock and the profile of an individual pressure pulse, it is possible to predict the decrease in hydrocarbon column height for each, essentially isolated, pulse. The combined effect of a series of these pulses can then be determined by compounding the results from each individual pulse.

References

Bruhn, R.L., Yonkee, W.A. and Parry, W.T. 1990 Structural and fluid-chemical properties of seismogenic normal faults. *Tectonophysics* **175**, 139–157.

Ge, S.M. and Garven, G. 1994 A theoretical model for thrust-induced deep groundwater expulsion with application to the Canadian Rocky mountains. *J. Geophys. Res. - Solid Earth* **99**, 13851–13868.

Hagiwara, T. and Iwata, T. 1968 Summary of the seismographic observation of Matsushiro swarm earthquakes. *Bull. Earthquake Res. Inst., Tokyo University* **46**, 485–515.

Holm, G.M. 1996 The central Graben: a dynamic overpressure system. In *AD1995: NW Europe's Hydrocarbon Industry*, eds. Glennie, K. and Hurst, A. Geological Society, London, 107–122.

Knipe, R.J. 1992 Faulting processes and fault seal. In *Structural and Tectonic Modelling and its Application to Petroleum Geology*, eds. Larsen, R. M., Brekke, H., Larsen, B. T. and Talleraas, E. Norsk Petroleums-Forening (Norwegian Petroleum Society), NPF Special Publication No. **1**. Amsterdam. Elsevier. 325–342.

Larson, R.M, Brekke, H., Larsen, B.T. and Talleraas, E. 1992 *Structural and Tectonic Modelling and its Application to Petroleum Geology*, Norsk Petroleums-Forening (Norwegian Petroleum Society), NPF Special Publication No. **1**. Amsterdam. Elsevier.

Lockner, D.A. and Byerlee, J.D. 1995 An earthquake instability model based on faults containing high fluid-pressure compartments. *Pure Appl. Geophys.* **145**, 717–745.

Parry, W.T. and Bruhn, R.L. 1990 Fluid pressure transients on seismogenic normal faults. *Tectonophysics* **179**, 335–344.

Scholz, C.H. 1989 Mechanics of faulting. *Annual Review of Earth and Planetary Sciences* **17**, 309–334.

Schowalter, T.T. 1979 Mechanics of secondary hydrocarbon migration and entrapment. *American Association of Petroleum Geologists Bulletin* **63**, 723–760.

Schwartz, D.P. and Coppersmith, K.J. 1984 Fault behaviour and characteristic earthquakes: Examples from the Wasatch and San Andreas fault zones. *J. Geophys. Res.* **89**, 5681–5698.

Sibson, R.H. 1981 Fluid flow accompanying faulting: field evidence and models. In *Earthquake Prediction: An International Review*, eds. Simpson, D.W. and Williams, P.G. American Geophysical Union, Maurice Ewing Series **4**. Washington. 593–603.

Sibson, R.H. 1989 Earthquake faulting as a structural process. *J. Structural Geology* **11**, 1–14.

Sibson, R.H. 1992 Implications of fault-valve behaviour for rupture nucleation and recurrence. *Tectonophysics* **211**, 283–293.

Sibson, R.H. 1996 Structural permeability of fault-fracture meshes. *J. Structural Geology* **18**, 1031–1042.